medRxiv preprint doi: https://doi.org/10.1101/2020.10.13.20212233; this version posted October 15, 2020. The copyright holder for this preprint (which was not certified by peer review) is the author/funder, who has granted medRxiv a license to display the preprint in perpetuity. It is made available under a CC-BY-NC 4.0 International license .

Heterogeneity in transmissibility and shedding SARS-CoV-2 via droplets and aerosols

Paul Z. Chen[1], Niklas Bobrovitz[2-4], Zahra Premji[5], Marion Koopmans[6], David N. Fisman[7,8], Frank X. Gu[1,9]*

[1]Department of Chemical Engineering & Applied Chemistry, University of Toronto, Toronto, Canada

[2]Temerty Faculty of Medicine, University of Toronto, Toronto, Canada

[3]Department of Critical Care Medicine, Cumming School of Medicine, University of Calgary, Calgary, Canada

[4]O'Brien Institute of Public Health, University of Calgary, Calgary, Canada

[5]Libraries & Cultural Resources, University of Calgary, Calgary, Canada

[6]Department of Viroscience, Erasmus University Medical Center, Rotterdam, Netherlands

[7]Division of Epidemiology, Dalla Lana School of Public Health, University of Toronto, Toronto, Canada

[8]Division of Infectious Diseases, Temerty Faculty of Medicine, University of Toronto, Toronto, Canada

[9]Institute of Biomedical Engineering, University of Toronto, Toronto, Canada

*Correspondence: f.gu@utoronto.ca

NOTE: This preprint reports new research that has not been certified by peer review and should not be used to guide clinical practice.

medRxiv preprint doi: https://doi.org/10.1101/2020.10.13.20212233; this version posted October 15, 2020. The copyright holder for this preprint
(which was not certified by peer review) is the author/funder, who has granted medRxiv a license to display the preprint in perpetuity.
It is made available under a CC-BY-NC 4.0 International license .

Abstract

A growing number of studies provide insight into how SARS-CoV-2 spreads[1-7]. Yet, many factors that characterize its transmissibility remain unclear, including mechanistic correlates of overdispersion, viral kinetics, the extent to which respiratory droplets and aerosols carry viable virus and the infectiousness of asymptomatic, presymptomatic and pediatric cases[7]. Here, we developed a comprehensive dataset of respiratory viral loads (rVLs) via systematic review and investigated these factors using meta-analyses and modeling. By comparing cases of COVID-19, SARS and influenza A(H1N1)pdm09, we found that heterogeneity in rVL was associated with overdispersion and facilitated the distinctions in individual variation in infectiousness among these emergent diseases. For COVID-19, case heterogeneity was broad throughout the infectious period, although rVL tended to peak at 1 day from symptom onset (DFSO) and be elevated for 1-5 DFSO. While most cases presented minimal risk, highly infectious ones could spread SARS-CoV-2 by talking, singing or breathing, which shed virions at comparable rates via droplets and aerosols. Coughing shed considerable quantities of virions, predominantly via droplets, and greatly increased the contagiousness of many symptomatic cases relative to asymptomatic ones. Asymptomatic and symptomatic infections showed similar likelihoods of expelling aerosols with SARS-CoV-2, as did adult and pediatric cases. Children tended to be less contagious by droplet spread than adults based on tendencies of symptomatology rather than rVL. Our findings address longstanding questions on SARS-CoV-2 transmissibility and present pertinent considerations for disease control.

medRxiv preprint doi: https://doi.org/10.1101/2020.10.13.20212233; this version posted October 15, 2020. The copyright holder for this preprint
(which was not certified by peer review) is the author/funder, who has granted medRxiv a license to display the preprint in perpetuity.
It is made available under a CC-BY-NC 4.0 International license .

Main body

The novel coronavirus SARS-CoV-2 has spread globally, causing the coronavirus disease 2019 (COVID-19) pandemic with more than 38.0 million infections and 1.0 million deaths (as of 13 October 2020)[8]. While the basic reproductive number has been estimated to be 2-3.6[1,2], transmissibility of SARS-CoV-2 is highly overdispersed, with numerous instances of superspreading[9-11] and few cases (10-20%) causing many secondary infections (80%)[4-6]. Estimates indicate 40-87% of cases are asymptomatic or paucisymptomatic, which facilitates transmission[2,3,12]. Infectiousness begins around -3 to -2 DFSO and has been estimated to last 8-10 DFSO[13-15]. Hence, the temporal infectiousness profile of COVID-19 resembles that of influenza[16], whereas its overdispersion is similar to that of severe acute respiratory syndrome (SARS)[17].

For respiratory virus transmission, airway epithelial cells shed virions to the extracellular fluid before atomization (from breathing, talking, singing, coughing and aerosol-generating procedures) partitions them into a polydisperse mixture of droplets (>5 μm) and aerosols (≤5 μm) that are expelled to the ambient environment[7]. Based on mass, droplets tend to settle gravitationally, whereas aerosols remain suspended and travel based on airflow profiles. Although proximity has been associated with infection risk for COVID-19[18], studies have also suggested that long-range aerosol spread occurs conditionally[9-11].

Despite these analyses, key factors that characterize the transmissibility of SARS-CoV-2 remain unclear. To investigate many of these factors, we synthesized evidence by systematic review, compared SARS-CoV-2 rVLs among subgroups, associated overdispersion, analyzed viral kinetics and modeled the likelihood of shedding viable virus via droplets and aerosols across respiratory activities, DFSO, case heterogeneity and subgroups. For inference on

medRxiv preprint doi: https://doi.org/10.1101/2020.10.13.20212233; this version posted October 15, 2020. The copyright holder for this preprint (which was not certified by peer review) is the author/funder, who has granted medRxiv a license to display the preprint in perpetuity. It is made available under a CC-BY-NC 4.0 International license .

transmissibility, we compared these analyses with those of SARS-CoV-1 (the most closely related human coronavirus) and A(H1N1)pdm09 (the most recent pandemic influenza virus), which spread by contact, droplets and aerosols[19,20].

Systematic review

To develop the comprehensive dataset, we conducted a systematic review on quantitative VL measurements for respiratory specimens taken during the infectious periods of SARS-CoV-2 (-3 to 10 DFSO)[13-15], SARS-CoV-1 (0-20 DFSO)[21] and A(H1N1)pdm09 (-2 to 9 DFSO)[16] (Methods). The systematic search (Supplementary Tables 1-5) identified 4,274 results. After screening and full-text review, 63 studies met the inclusion criteria and were used for analysis (Fig. 1) (n=9,692 total specimens), which included adult (n=5,124) and pediatric (n=1,593) cases and measurements for asymptomatic (n=2,378), presymptomatic (n=28) and symptomatic (n=7,231) infections. According to a hybrid Joanna Briggs Institute critical appraisal checklist, risk of bias was low to moderate for included studies (Extended Data Table 1).

Meta-analysis and subgroup analyses of rVL

For each study in the systematic dataset, we used specimen concentrations to estimate rVLs (Methods). We then performed a random-effects meta-analysis (Extended Data Fig. 1), which showed that, during the infectious periods, the expected rVL of SARS-CoV-2 was comparable to that of SARS-CoV-1 (p=0.148, two-sided Welch's t-test) but lesser than that of A(H1N1)pdm09 (p<0.0001). We also performed random-effects subgroup analyses for COVID-19 (Fig. 2), which showed that expected SARS-CoV-2 rVLs were consistent between pediatric and adult cases (p=0.861) and between symptomatic/presymptomatic and asymptomatic infections (p=0.951).

medRxiv preprint doi: https://doi.org/10.1101/2020.10.13.20212233; this version posted October 15, 2020. The copyright holder for this preprint (which was not certified by peer review) is the author/funder, who has granted medRxiv a license to display the preprint in perpetuity. It is made available under a CC-BY-NC 4.0 International license .

87

88 **Association of heterogeneity in rVL with overdispersion**

89 Since few cases drive the transmission of SARS-CoV-2 (dispersion parameter *k*, 0.10-0.58)[4-6]
90 and SARS-CoV-1 (*k*, 0.16-0.17)[17] whereas A(H1N1)pdm09 (*k*, 7.4-14.4)[22,23] spreads more
91 homogeneously, we sought to find a mechanistic association for overdispersion. As an empirical
92 estimate, *k* depends on myriad extrinsic (behavioral, environmental and invention) and host (host
93 defenses) factors. However, since dispersion is similar across distinct outbreaks of a virus[17], we
94 hypothesized that an intrinsic virological factor mediates *k* for these emergent respiratory
95 infections.

96 We assessed heterogeneity in rVL. For all three viruses, rVLs best conformed to Weibull
97 distributions (Extended Data Fig. 2), and we fitted the entirety of individual sample data for each
98 virus in the systematic dataset (Fig. 3a, Extended Data Fig. 2n). While COVID-19 and SARS
99 cases tended to shed lesser virus than those with A(H1N1)pdm09 (Extended Data Fig. 1), broad
100 heterogeneity in rVL inverted this relationship for highly infectious individuals (Extended Data
101 Fig. 3a-c). At the 90th case percentile (cp), the estimated rVL was 8.91 (8.82-9.00, 95%
102 confidence interval [CI]) $\log_{10}$ copies/ml for SARS-CoV-2, whereas it was 8.62 (8.47-8.76) $\log_{10}$
103 copies/ml for A(H1N1)pdm09. Moreover, heterogeneity in rVL was similar among adult,
104 pediatric, symptomatic/presymptomatic and asymptomatic COVID-19 cases (Extended Data Fig.
105 3d-g), with standard deviations (SDs) of 2.01-2.06 $\log_{10}$ copies/ml (Extended Data Table 2).

106 To investigate the relationship between *k* and heterogeneity in rVL, we performed a meta-
107 regression using each included study (Fig. 3b). The analysis showed a negative association
108 (p=0.031, meta-regression slope t-test), indicating that heterogeneity in rVL intrinsically
109 facilitated the distinctions in overdispersion among the emergent infections.

medRxiv preprint doi: https://doi.org/10.1101/2020.10.13.20212233; this version posted October 15, 2020. The copyright holder for this preprint
(which was not certified by peer review) is the author/funder, who has granted medRxiv a license to display the preprint in perpetuity.
It is made available under a CC-BY-NC 4.0 International license .

Kinetics of SARS-CoV-2 rVL

To investigate dynamics, we delineated SARS-CoV-2 rVLs by DFSO and fitted the mean estimates to a mechanistic epithelial cell-limited model for viral kinetics (Fig. 3c, Methods). The outputs indicated that, on average, each productively infected cell in the airway epithelium shed SARS-CoV-2 at 1.11 (0.51-1.71, 95% CI) copies/ml day^{-1} and infected up to 10.6 susceptible cells (Extended Data Table 3). The turnover rate for infected epithelial cells was 0.55 (0.23-0.87) $days^{-1}$, while the half-life of SARS-CoV-2 in the respiratory tract was 4.35 (2.23-97.8) hours. By extrapolating the model to an initial rVL of 0-1 log_{10} copies/ml, the estimated incubation period was 5.38-4.52 days, which agrees with epidemiological findings[1]. Conversely, the expected duration of shedding was 26.8 DFSO. Thus, SARS-CoV-2 replicated exponentially in the respiratory tract based on a mean rate constant of 4.02×10^{-7} (3.01×10^{-7}-5.03×10^{-7}) $(copies/ml)^{-1}$ day^{-1} after infection. Around 1 DFSO, rVL peaked, as the number of infected epithelial cells reached equilibrium, and then diminished exponentially.

As SARS-CoV-2 rVLs showed widespread heterogeneity across the infectious period, we fitted distributions for each DFSO (Fig. 3d), which showed that high rVLs also increased from the presymptomatic period before decreasing towards the end of the first week of illness. At the 90^{th} cp, SARS-CoV-2 rVL peaked at 1 DFSO at 9.83 (9.12-10.61) log_{10} copies/ml, an order of magnitude greater than the overall 90^{th}-cp estimate (Extended Data Table 2). The estimate remained ≥9.33 log_{10} copies/ml between 1-5 DFSO. At -1 DFSO, the 90^{th}-cp rVL was 8.30 (6.88-10.02) log_{10} copies/ml, while it was 7.92 (7.34-8.55) log_{10} copies/ml at 10 DFSO (Extended Data Fig. 3h-s).

medRxiv preprint doi: https://doi.org/10.1101/2020.10.13.20212233; this version posted October 15, 2020. The copyright holder for this preprint
(which was not certified by peer review) is the author/funder, who has granted medRxiv a license to display the preprint in perpetuity.
It is made available under a CC-BY-NC 4.0 International license .

Likelihood of droplets and aerosols containing virions

Since rVL is an intensive quantity, the volume fraction of virions is low and viral partitioning coincides with atomization, we used Poisson statistics to model likelihood profiles. To calculate an unbiased estimator of partitioning (the expected number of viable copies per particle), our method multiplied rVL estimates with the volumes of atomized particles and an assumed viability proportion of 0.1% after dehydration (Methods).

When expelled by the mean COVID-19 case across the infectious period, respiratory particles showed minimal likelihoods of carrying viable SARS-CoV-2 (Fig. 4a,b). Aerosols (dehydrated aerodynamic diameter [d_a]≤5 μm) were <0.001% likely to contain a virion. Droplets also had low likelihoods: at d_a=40 μm, they were ≤0.4% likely to contain a virion.

COVID-19 cases with high rVLs, however, expelled particles with considerably greater likelihoods of carrying viable copies (Fig. 4a,b). For the 98th cp at 1 DFSO, 18.2% (8.8-27.6%) of aerosols (d_a=5 μm) contained at least one SARS-CoV-2 virion. For d_a>14.4 μm, droplets were >99% likely to contain virions, with large ones carrying tens to hundreds.

Shedding SARS-CoV-2 via respiratory activities

Using the partitioning estimates in conjunction with published profiles of the particles expelled by respiratory activities (Extended Data Fig. 4), we modeled the rates at which talking, singing, breathing and coughing shed viable SARS-CoV-2 across d_a (Fig. 4c-f). Among the non-presenting activities, singing emitted virions most rapidly followed by talking and then breathing, although talking loudly was similar to singing (Extended Data Fig. 4c,d). These activities produced more aerosols than droplets, but particle size correlated with the likelihood of containing virions. Thus, talking, singing and breathing shed SARS-CoV-2 at similar rates via

medRxiv preprint doi: https://doi.org/10.1101/2020.10.13.20212233; this version posted October 15, 2020. The copyright holder for this preprint (which was not certified by peer review) is the author/funder, who has granted medRxiv a license to display the preprint in perpetuity. It is made available under a CC-BY-NC 4.0 International license .

aerosols and droplets: aerosols mediated 25.2-43.4% of the virions expelled by the non-presenting activities (Fig. 4g). In comparison, coughing shed far greater quantities of virions (Fig. 4f), of which >99.9% were carried by droplets.

We further examined the influences of case heterogeneity and disease course on expelling SARS-CoV-2 (Fig. 4h, Extended Data Fig. 5). The estimated total shedding rates (over all particle sizes) for a respiratory activity spanned ≥8.55 orders of magnitude on each DFSO; cumulatively from -1 to 10 DFSO, they spanned 11.2 orders of magnitude. Hence, most cases expelled a negligible number of SARS-CoV-2 virions by talking, singing or breathing. Shedding occurred most rapidly at 1 DFSO: for the 98th cp, singing discharged 31.5 (3.26-379, 95% CI) virions/min to the ambient environment, while talking emitted 4.67 (0.48-56.1) virions/min and breathing exhaled 1.27 (0.13-15.2) virions/min; these estimates were two orders of magnitude greater than those for the 86th cp. For the 98th cp at -1 DFSO, singing shed 1.31 (0.01-406) virions/min and breathing exhaled 5.24×10^{-2} (5.28×10^{-4}-16.3) virions/min. The estimates at 7-10 DFSO were comparable to these presymptomatic ones (Fig. 4h, Extended Data Fig. 5).

At 1 DFSO, coughing expelled 2.13×10^{6} (2.20×10^{5}-2.56×10^{7}) virions/cough for the 98th cp, 90.4 (24.6-372) virions/cough for the 50th cp and 2.66 (0.65-13.1) virions/cough for the 25th cp (Extended Data Fig. 5c). At -1 and 10 DFSO, these estimates were reduced by ~2 orders of magnitude. Thus, most symptomatic cases shed considerable quantities of SARS-CoV-2 by coughing; a single cough accounted for the virions emitted by weeks of singing for a case.

As indicated by similar mean rVLs (Fig. 2) and heterogeneities in rVL (Extended Data Table 2), asymptomatic, symptomatic/presymptomatic, adult and pediatric COVID-19 cases showed similar profiles for total shedding rates (Extended Fig. 6a-d). The estimates showed that the top 6.1%, 2.4% and 1.1% of pediatric cases shed ≥1 virion/min by singing, talking and

medRxiv preprint doi: https://doi.org/10.1101/2020.10.13.20212233; this version posted October 15, 2020. The copyright holder for this preprint (which was not certified by peer review) is the author/funder, who has granted medRxiv a license to display the preprint in perpetuity. It is made available under a CC-BY-NC 4.0 International license .

179 breathing, respectively, while 62.5% expelled ≥10 virions/cough. In general, highly infectious
180 COVID-19 cases expelled virions more rapidly than did ones with A(H1N1)pdm09 (Extended
181 Data Fig. 6f).
182
183 **Discussion**
184 This study provided comprehensive, systematic analyses of several factors characterizing the
185 transmissibility of SARS-CoV-2. First, we evaluated the influence of heterogeneity in rVL. Our
186 findings show that broad heterogeneity in rVL facilitates greater variation in individual
187 infectiousness in the COVID-19 pandemic than was found in the 2009 H1N1 pandemic. For each
188 respiratory activity, SARS-CoV-2 shedding rates span >11 orders of magnitude throughout the
189 infectious period. While most COVID-19 cases present minimal transmission risk by talking,
190 singing or breathing, highly infectious ones, including asymptomatic and presymptomatic
191 infections, can spread SARS-CoV-2 through these activities. Our model estimates, when
192 corrected to copies rather than virions, align with recent clinical findings for exhalation rates of
193 SARS-CoV-2[24]. Moreover, the findings suggest that heterogeneity in rVL may be a virological
194 factor generally associated with overdispersion for respiratory infections. In this case, rVL
195 distribution may serve as an early correlate for transmission patterns, including superspreading,
196 during outbreaks of novel respiratory viruses, providing insight for disease control before large-
197 scale epidemiological analyses empirically characterize *k*.
198 Second, we analyzed SARS-CoV-2 kinetics during respiratory infection. While
199 heterogeneity remains broad throughout the infectious period, the systematic dataset indicates
200 that rVL tends to peak at 1 DFSO and be elevated for 1-5 DFSO, coinciding with the period of
201 highest attack rates observed among close contacts[25]. These results indicate that transmission risk

medRxiv preprint doi: https://doi.org/10.1101/2020.10.13.20212233; this version posted October 15, 2020. The copyright holder for this preprint (which was not certified by peer review) is the author/funder, who has granted medRxiv a license to display the preprint in perpetuity. It is made available under a CC-BY-NC 4.0 International license .

tends to be greatest soon after illness rather than in the presymptomatic period, which concurs with large tracing studies (6.4-12.6% of secondary infections from presymptomatic transmission)[26,27] rather than early temporal models (~44%)[14]. Furthermore, our kinetic analysis suggests that, on average, SARS-CoV-2 reaches diagnostic concentrations 1.60-3.22 days after respiratory infection (-3.78 to -2.16 DFSO), assuming assay detection limits of 1-3 $\log_{10}$ copies/ml, respectively, for nasopharyngeal swabs immersed in 1 ml of transport media.

Third, we modeled the likelihood of shedding SARS-CoV-2 via aerosols. Talking, singing and breathing shed SARS-CoV-2 at comparable rates through droplets and aerosols (up to tens to hundreds of virions/min). As airborne spread is recognized as a key mode of transmission for A(H1N1)pdm09[20], our model estimates and comparative analyses support, particularly for highly infectious cases, airborne spread as a transmission mode for SARS-CoV-2. While our models delineated aerosols from droplets at the classical threshold (d_a=5 µm), recent reports show that, based on emission vectors and environmental conditions, respiratory particles larger than 5 µm can also travel >2 m in air[28,29], further supporting the plausibility of the airborne transmission of SARS-CoV-2. However, with short durations of stay in well-ventilated areas, the concentration, and exposure risk, of aerosols remains correlated with proximity to infectious cases[18,28].

Fourth, we assessed the relative infectiousness of COVID-19 subgroups. Since rVL distributions are similar among subgroups and the predominant source of aerosols is the non-presenting respiratory activities (talking, singing and breathing), symptomatic and asymptomatic infections present similar risks for aerosol spread, as do adult and pediatric cases. However, most cases shed considerable numbers of virions via large droplets by coughing, a common symptom of COVID-19[30]. Thus, symptomatic infections tend to be significantly more contagious than asymptomatic ones, providing a reason as to why asymptomatic cases transmit SARS-CoV-2 at

medRxiv preprint doi: https://doi.org/10.1101/2020.10.13.20212233; this version posted October 15, 2020. The copyright holder for this preprint (which was not certified by peer review) is the author/funder, who has granted medRxiv a license to display the preprint in perpetuity. It is made available under a CC-BY-NC 4.0 International license .

lower relative rates[3], especially in close contact[31], despite similar rVLs and increased contact patterns. Accordingly, children (48-54% of symptomatic cases present with cough)[32,33] tend to be less contagious by droplet spread than adults (68-80%)[30,33] based on tendencies of symptomatology rather than rVL.

Our study has limitations. The systematic search found a limited number of studies reporting quantitative specimen measurements from the presymptomatic period, meaning these estimates may be sensitive to sampling bias. Although additional studies have reported semiquantitative metrics (cycle thresholds), these data were excluded because they cannot be compared on an absolute scale due to batch effects[34], limiting use in compound analyses. Furthermore, our analyses considered population-level estimates of the infectious periods and viability proportions, which omit individual variation in the dynamics of virus viability. Some patients shed SARS-CoV-2 with diminishing viability soon after symptom onset[13], while others produce replication-competent virus for weeks[35]. It remains unelucidated how case characteristics and environmental factors affect the viability dynamics of SARS-CoV-2.

Taken together, our findings provide a potential path forward for disease control. They highlight the disproportionate role of high-risk cases, settings and circumstances in propelling the COVID-19 pandemic. Since highly infectious cases, regardless of age or symptomatology, can rapidly shed SARS-CoV-2 via both droplets and aerosols, airborne spread should also be recognized as a transmission risk, including for superspreading. Strategies to abate infection should limit crowd numbers and duration of stay while reinforcing distancing and then widespread mask usage; well-ventilated settings can be recognized as lower risk venues. Coughing sheds considerable quantities of virions for most infections, while rVL tends to peak at 1 DFSO and can be high throughout the infectious period. Thus, immediate, sustained self-

medRxiv preprint doi: https://doi.org/10.1101/2020.10.13.20212233; this version posted October 15, 2020. The copyright holder for this preprint
(which was not certified by peer review) is the author/funder, who has granted medRxiv a license to display the preprint in perpetuity.
It is made available under a CC-BY-NC 4.0 International license .

248 isolation upon symptom presentation is crucial to curb transmission from symptomatic cases.
249 While diagnosing COVID-19, qRT-PCR can also help to triage contact tracing, prioritizing
250 patients with higher specimen measurements: for nasopharyngeal swabs immersed in 1 ml of
251 transport media, ≥7.14 (7.07-7.22, 95% CI) $\log_{10}$ copies/ml corresponds to ≥80^{th} cp. Doing so
252 may identify asymptomatic and presymptomatic cases more efficiently, a key step towards
253 mitigation as the pandemic continues.

medRxiv preprint doi: https://doi.org/10.1101/2020.10.13.20212233; this version posted October 15, 2020. The copyright holder for this preprint
(which was not certified by peer review) is the author/funder, who has granted medRxiv a license to display the preprint in perpetuity.
It is made available under a CC-BY-NC 4.0 International license .

References

1 Li, Q. *et al.* Early transmission dynamics in Wuhan, China, of novel coronavirus-infected pneumonia. *N. Engl. J. Med.* **382**, 1199-1207, doi:10.1056/NEJMoa2001316 (2020).

2 Hao, X. *et al.* Reconstruction of the full transmission dynamics of COVID-19 in Wuhan. *Nature* **584**, 420-424, doi:10.1038/s41586-020-2554-8 (2020).

3 Li, R. *et al.* Substantial undocumented infection facilitates the rapid dissemination of novel coronavirus (SARS-CoV-2). *Science* **368**, 489-493, doi:10.1126/science.abb3221 (2020).

4 Endo, A., Abbott, S., Kucharski, A. J. & Funk, S. Estimating the overdispersion in COVID-19 transmission using outbreak sizes outside China. *Wellcome Open Research* **5**, doi:10.12688/wellcomeopenres.15842.1 (2020).

5 Laxminarayan, R. *et al.* Epidemiology and transmission dynamics of COVID-19 in two Indian states. *Science*, eabd7672, doi:10.1126/science.abd7672 (2020).

6 Bi, Q. *et al.* Epidemiology and transmission of COVID-19 in 391 cases and 1286 of their close contacts in Shenzhen, China: a retrospective cohort study. *Lancet Infect. Dis.* **20**, 911-919, doi:10.1016/s1473-3099(20)30287-5 (2020).

7 Organization, W. H. Transmission of SARS-CoV-2: implications for infection prevention precautions (scientific brief). July 9, 2020.

8 Dong, E., Du, H. & Gardner, L. An interactive web-based dashboard to track COVID-19 in real time. *Lancet Infect. Dis.* **20**, 533-534, doi:10.1016/S1473-3099(20)30120-1 (2020).

9 Shen, Y. *et al.* Community outbreak investigation of SARS-CoV-2 transmission among bus riders in Eastern China. *JAMA Intern. Med.*, doi:10.1001/jamainternmed.2020.5225 (2020).

medRxiv preprint doi: https://doi.org/10.1101/2020.10.13.20212233; this version posted October 15, 2020. The copyright holder for this preprint (which was not certified by peer review) is the author/funder, who has granted medRxiv a license to display the preprint in perpetuity. It is made available under a CC-BY-NC 4.0 International license .

10 Lu, J. *et al.* COVID-19 outbreak associated with air conditioning in restaurant, Guangzhou, China, 2020. *Emerg. Infect. Dis.* **26**, 1628-1631, doi:10.3201/eid2607.200764 (2020).

11 Hamner, L. *et al.* High SARS-CoV-2 attack rate following exposure at a choir practice - Skagit County, Washington, March 2020. *MMWR Morb. Mortal. Wkly. Rep.* **69**, 606-610, doi:10.15585/mmwr.mm6919e6 (2020).

12 Oran, D. P. & Topol, E. J. Prevalence of asymptomatic SARS-CoV-2 infection: a narrative review. *Ann. Intern. Med.* **173**, 362-367, doi:10.7326/M20-3012 (2020).

13 Wolfel, R. *et al.* Virological assessment of hospitalized patients with COVID-2019. *Nature* **581**, 465-469, doi:10.1038/s41586-020-2196-x (2020).

14 He, X. *et al.* Temporal dynamics in viral shedding and transmissibility of COVID-19. *Nat. Med.* **26**, 672-675, doi:10.1038/s41591-020-0869-5 (2020).

15 Arons, M. M. *et al.* Presymptomatic SARS-CoV-2 infections and transmission in a skilled nursing facility. *N. Engl. J. Med.* **382**, 2081-2090, doi:10.1056/NEJMoa2008457 (2020).

16 Ip, D. K. *et al.* Viral shedding and transmission potential of asymptomatic and paucisymptomatic influenza virus infections in the community. *Clin. Infect. Dis.* **64**, 736-742, doi:10.1093/cid/ciw841 (2017).

17 Lloyd-Smith, J. O., Schreiber, S. J., Kopp, P. E. & Getz, W. M. Superspreading and the effect of individual variation on disease emergence. *Nature* **438**, 355-359, doi:10.1038/nature04153 (2005).

18 Chu, D. K. *et al.* Physical distancing, face masks, and eye protection to prevent person-to-person transmission of SARS-CoV-2 and COVID-19: a systematic review and meta-analysis. *Lancet* **395**, 1973-1987, doi:10.1016/S0140-6736(20)31142-9 (2020).

medRxiv preprint doi: https://doi.org/10.1101/2020.10.13.20212233; this version posted October 15, 2020. The copyright holder for this preprint
(which was not certified by peer review) is the author/funder, who has granted medRxiv a license to display the preprint in perpetuity.
It is made available under a CC-BY-NC 4.0 International license .

19 Yu, I. T. *et al.* Evidence of airborne transmission of the severe acute respiratory syndrome virus. *N. Engl. J. Med.* **350**, 1731-1739, doi:10.1056/NEJMoa032867 (2004).

20 Cowling, B. J. *et al.* Aerosol transmission is an important mode of influenza A virus spread. *Nat. Commun.* **4**, 1935, doi:10.1038/ncomms2922 (2013).

21 Pitzer, V. E., Leung, G. M. & Lipsitch, M. Estimating variability in the transmission of severe acute respiratory syndrome to household contacts in Hong Kong, China. *Am. J. Epidemiol.* **166**, 355-363, doi:10.1093/aje/kwm082 (2007).

22 Roberts, M. G. & Nishiura, H. Early estimation of the reproduction number in the presence of imported cases: pandemic influenza H1N1-2009 in New Zealand. *PLoS One* **6**, e17835, doi:10.1371/journal.pone.0017835 (2011).

23 Brugger, J. & Althaus, C. L. Transmission of and susceptibility to seasonal influenza in Switzerland from 2003 to 2015. *Epidemics* **30**, 100373, doi:10.1016/j.epidem.2019.100373 (2020).

24 Ma, J. *et al.* COVID-19 patients in earlier stages exhaled millions of SARS-CoV-2 per hour. *Clin. Infect. Dis.*, doi:10.1093/cid/ciaa1283 (2020).

25 Cheng, H. Y. *et al.* Contact tracing assessment of COVID-19 transmission dynamics in Taiwan and risk at different exposure periods before and after symptom onset. *JAMA Intern. Med.*, doi:10.1001/jamainternmed.2020.2020 (2020).

26 Wei, W. E. *et al.* Presymptomatic transmission of SARS-CoV-2 — Singapore, January 23-March 16, 2020. *MMWR Morb. Mortal. Wkly. Rep.* **69**, 411-415, doi:10.15585/mmwr.mm6914e1 (2020).

27 Du, Z. *et al.* Serial interval of COVID-19 among publicly reported confirmed cases. *Emerg. Infect. Dis.* **26**, 1341-1343, doi:10.3201/eid2606.200357 (2020).

medRxiv preprint doi: https://doi.org/10.1101/2020.10.13.20212233; this version posted October 15, 2020. The copyright holder for this preprint
(which was not certified by peer review) is the author/funder, who has granted medRxiv a license to display the preprint in perpetuity.
It is made available under a CC-BY-NC 4.0 International license .

28 Abkarian, M., Mendez, S., Xue, N., Yang, F. & Stone, H. A. Speech can produce jet-like transport relevant to asymptomatic spreading of virus. *Proc. Natl. Acad. Sci. U. S. A.*, doi:10.1073/pnas.2012156117 (2020).

29 Bourouiba, L. Turbulent gas clouds and respiratory pathogen emissions: potential implications for reducing transmission of COVID-19. *JAMA* **323**, 1837-1838, doi:10.1001/jama.2020.4756 (2020).

30 Guan, W. J. *et al.* Clinical characteristics of coronavirus disease 2019 in China. *N. Engl. J. Med.* **382**, 1708-1720, doi:10.1056/NEJMoa2002032 (2020).

31 Luo, L. *et al.* Contact settings and risk for transmission in 3410 close contacts of patients with COVID-19 in Guangzhou, China: a prospective cohort study. *Ann. Intern. Med.*, doi:10.7326/M20-2671 (2020).

32 Lu, X. *et al.* SARS-CoV-2 infection in children. *N. Engl. J. Med.* **382**, 1663-1665, doi:10.1056/NEJMc2005073 (2020).

33 CDC COVID-19 Response Team. Coronavirus disease 2019 in children - United States, February 12-April 2, 2020. *MMWR Morb. Mortal. Wkly. Rep.* **69**, 422-426, doi:10.15585/mmwr.mm6914e4 (2020).

34 Han, M. S., Byun, J. H., Cho, Y. & Rim, J. H. RT-PCR for SARS-CoV-2: quantitative versus qualitative. *Lancet Infect. Dis.*, doi:10.1016/S1473-3099(20)30424-2 (2020).

35 van Kampen, J. J. A. *et al.* Shedding of infectious virus in hospitalized patients with coronavirus disease-2019 (COVID-19): duration and key determinants. Preprint at medRxiv doi:10.1101/2020.06.08.20125310 (2020).

medRxiv preprint doi: https://doi.org/10.1101/2020.10.13.20212233; this version posted October 15, 2020. The copyright holder for this preprint
(which was not certified by peer review) is the author/funder, who has granted medRxiv a license to display the preprint in perpetuity.
It is made available under a CC-BY-NC 4.0 International license .

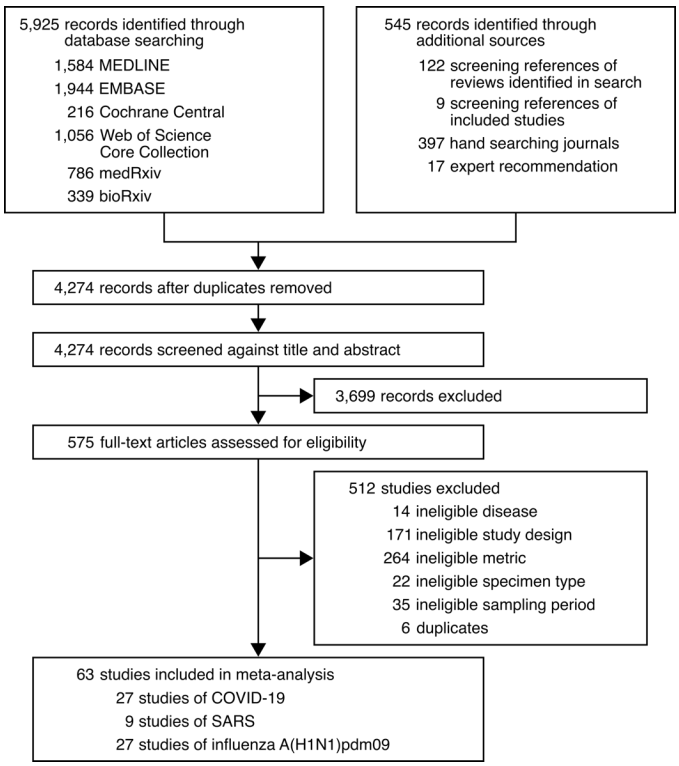

342

343 **Fig. 1. Development of the systematic dataset.**

medRxiv preprint doi: https://doi.org/10.1101/2020.10.13.20212233; this version posted October 15, 2020. The copyright holder for this preprint (which was not certified by peer review) is the author/funder, who has granted medRxiv a license to display the preprint in perpetuity. It is made available under a CC-BY-NC 4.0 International license .

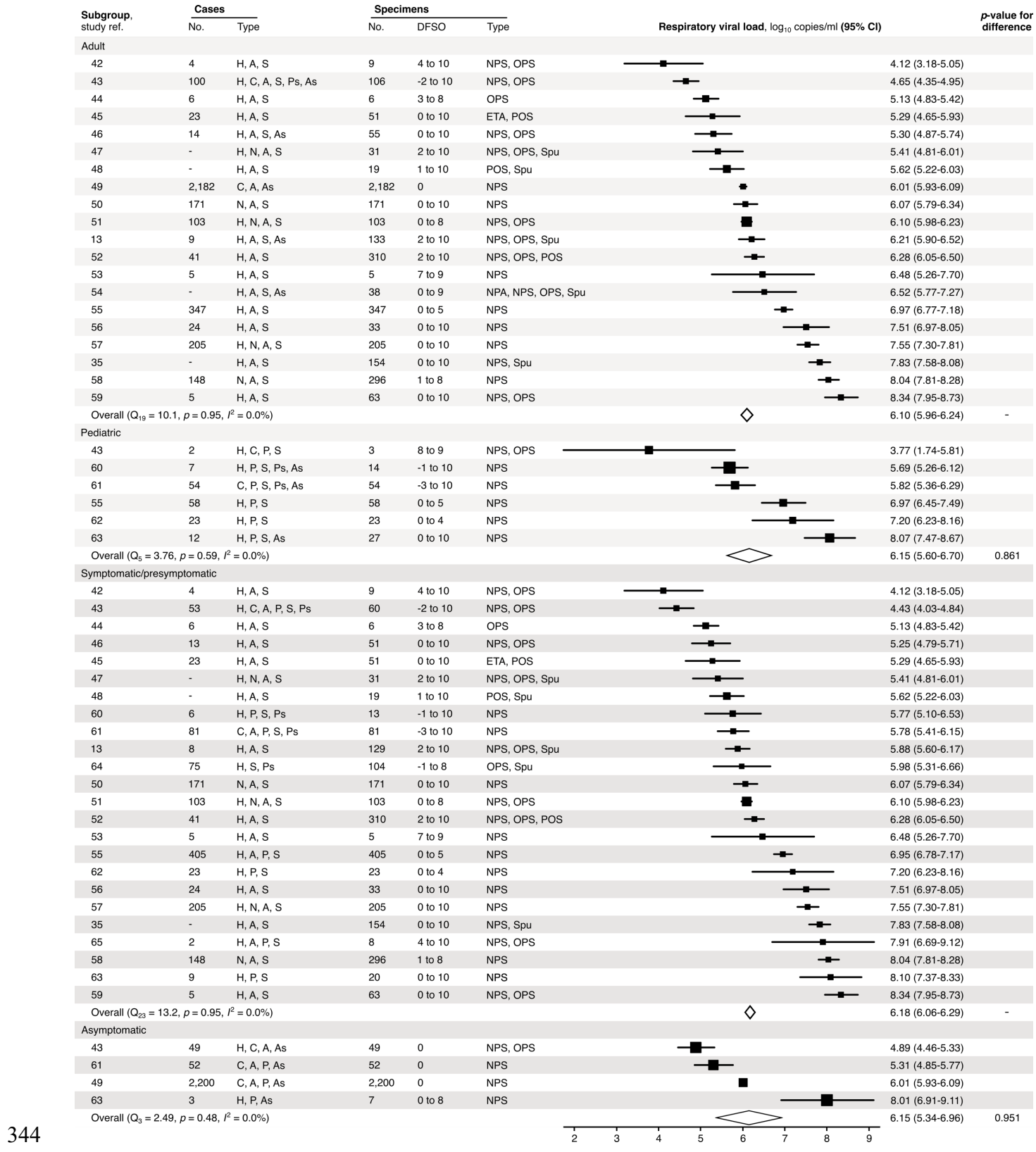

344

medRxiv preprint doi: https://doi.org/10.1101/2020.10.13.20212233; this version posted October 15, 2020. The copyright holder for this preprint
(which was not certified by peer review) is the author/funder, who has granted medRxiv a license to display the preprint in perpetuity.
It is made available under a CC-BY-NC 4.0 International license .

Fig. 2. Subgroup analyses of SARS-CoV-2 respiratory viral load during the infectious period. Random-effects meta-analyses comparing the expected rVLs of adult (>18 years old) COVID-19 cases with pediatric (≤18 years old) ones (top) and symptomatic/presymptomatic infections with asymptomatic ones (bottom) during the infectious period. Quantitative specimen measurements were used to estimate rVLs, which refer to virus concentrations in the respiratory tract. Case types: hospitalized (H), not admitted (N), community (C), adult (A), pediatric (P), symptomatic (S), presymptomatic (Ps) and asymptomatic (As). Specimen types: endotracheal aspirate (ETA), nasopharyngeal aspirate (NPA), nasopharyngeal swab (NPS), oropharyngeal swab (OPS), posterior oropharyngeal saliva (POS) and sputum (Spu). Studies after ref. 35 are listed in Methods. Dashes denote case numbers that were not obtained. Box sizes are proportional to weighting in the overall estimates. Two-sided Welch's *t*-tests, non-significance ($p>0.05$).

medRxiv preprint doi: https://doi.org/10.1101/2020.10.13.20212233; this version posted October 15, 2020. The copyright holder for this preprint
(which was not certified by peer review) is the author/funder, who has granted medRxiv a license to display the preprint in perpetuity.
It is made available under a CC-BY-NC 4.0 International license .

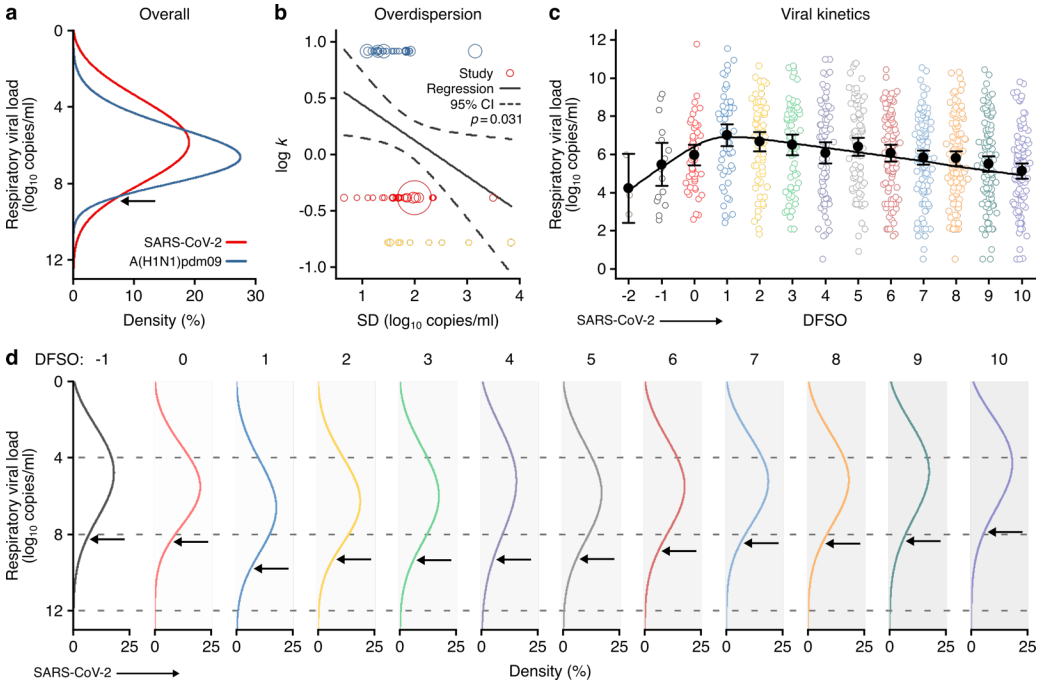

Fig. 3. Heterogeneity and kinetics of SARS-CoV-2 respiratory viral load. a, Estimated distribution of rVL for SARS-CoV-2 (n=3,778 samples from n=24 studies) and A(H1N1)pdm09 (n=512 samples from n=10 studies) throughout the infectious periods. **b,** Meta-regression of dispersion parameter (k) with the standard deviation (SD) of rVLs from included studies (r=-0.27). Estimates of k were pooled from the literature. Red, yellow and blue circles denote COVID-19 (n=27), SARS (n=9) and A(H1N1)pdm09 (n=27) studies, respectively. Circle sizes are proportional to weighting in the meta-regression. The p-value was obtained using the meta-regression slope t-test. **c,** SARS-CoV-2 rVLs fitted to a mechanistic model of viral kinetics (black curve, r^2=0.88). Filled circles and bars depict mean estimates and 95% CIs. Open circles show the entirety of individual sample data over DFSO (left to right, n=3, 15, 48, 59, 69, 71, 81, 87, 102, 125, 119, 117 and 110 samples from n=19 studies). **d,** Estimated distributions of SARS-CoV-2 rVL over DFSO. Earlier DFSO were excluded based on limited data. Weibull distributions were fitted on the entirety of individual sample data for the virus (**a**) or DFSO (**d**) in the systematic dataset. Arrows denote 90th case percentiles for SARS-CoV-2 rVL.

medRxiv preprint doi: https://doi.org/10.1101/2020.10.13.20212233; this version posted October 15, 2020. The copyright holder for this preprint
(which was not certified by peer review) is the author/funder, who has granted medRxiv a license to display the preprint in perpetuity.
It is made available under a CC-BY-NC 4.0 International license .

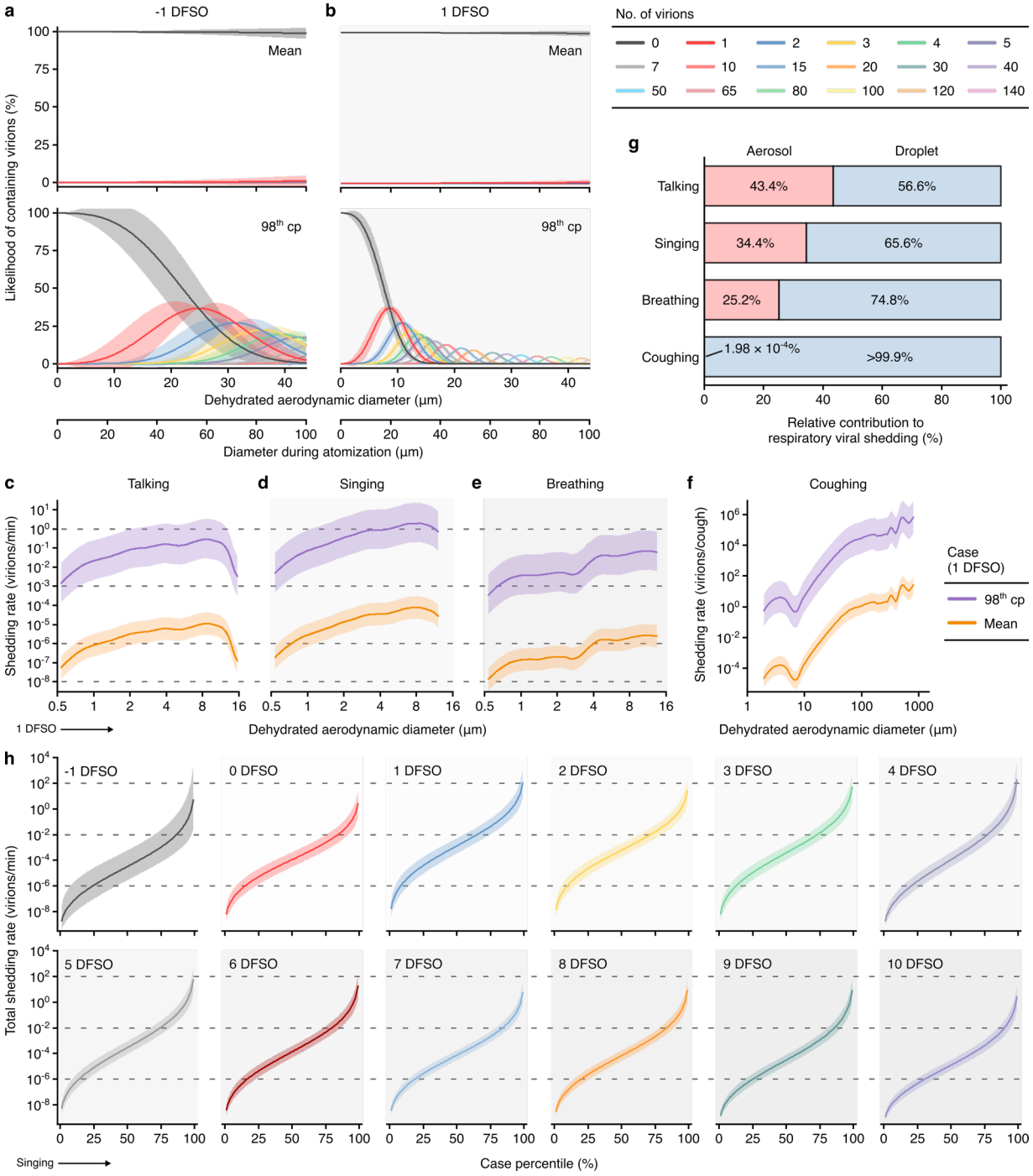

Fig. 4. Heterogeneity in shedding SARS-CoV-2 via droplets and aerosols. a,b, Likelihood of respiratory particles containing viable SARS-CoV-2 when expelled by the mean (top) or 98th case percentile (cp) (bottom) COVID-19 cases at -1 (**a**) or 1 (**b**) DFSO. The models considered virus viability within dehydrated particles. Diameters during atomization were included to show

medRxiv preprint doi: https://doi.org/10.1101/2020.10.13.20212233; this version posted October 15, 2020. The copyright holder for this preprint
(which was not certified by peer review) is the author/funder, who has granted medRxiv a license to display the preprint in perpetuity.
It is made available under a CC-BY-NC 4.0 International license .

their size relationship with dehydrated aerodynamic diameter (d_a), but not likelihood of containing virions during atomization. For higher no. of virions, some likelihood curves were omitted to aid visualization. When the likelihood for 0 virions approaches 0%, particles are expected to contain at least one viable copy. **c-f**, Rate that the mean and 98th-cp COVID-19 cases at 1 DFSO shed viable SARS-CoV-2 by talking (**c**), singing (**d**), breathing (**e**) or coughing (**f**) over d_a. **g**, Relative contribution of aerosols ($d_a \leq 5$ μm, red bar) and droplets ($d_a > 5$ μm, blue bar) to shedding virions for the respiratory activities. **h**, Case heterogeneity in the total shedding rate (over all particle sizes) of virions via singing across the infectious period. Earlier presymptomatic days were excluded based on limited data. Data range between the 1st and 99th cps. Lines and bands represent estimates and 95% CIs, respectively, for likelihoods or Poisson means.

medRxiv preprint doi: https://doi.org/10.1101/2020.10.13.20212233; this version posted October 15, 2020. The copyright holder for this preprint (which was not certified by peer review) is the author/funder, who has granted medRxiv a license to display the preprint in perpetuity. It is made available under a CC-BY-NC 4.0 International license .

Methods

Search strategy, selection criteria and data collection

We undertook a systematic review and prospectively submitted the systematic review protocol for registration on PROSPERO (registration number, CRD42020204637). Other than the title of this study, we have followed PRISMA reporting guidelines[36]. The systematic review was conducted according to Cochrane methods guidance[37].

The search included papers that (i) reported positive, quantitative measurements (copies/ml or an equivalent metric) of SARS-CoV-2, SARS-CoV-1 or A(H1N1)pdm09 in human respiratory specimens (ETA, NPA, NPS, OPS, POS and Spu) from COVID-19, SARS or A(H1N1)pdm09 cases; (ii) reported data that could be extracted from the infectious periods of SARS-CoV-2 (defined as -3 to +10 DFSO for symptomatic cases and 0 to +10 days from the day of laboratory diagnosis for asymptomatic cases), SARS-CoV-1 (defined as 0 to +20 DFSO or the equivalent asymptomatic period) or A(H1N1)pdm09 (defined as -2 to +9 DFSO for symptomatic cases and 0 days to +9 days from the day of laboratory diagnosis for asymptomatic cases); and (iii) reported data for two or more cases with laboratory-confirmed COVID-19, SARS or A(H1N1)pdm09. Quantitative specimen measurements were considered after RNA extraction for diagnostic sequences of SARS-CoV-2 (*Ofr1b*, *N*, *RdRp* and *E* genes), SARS-CoV-1 (*Ofr1b*, *N* and *RdRp* genes) and A(H1N1)pdm09 (*HA* and *M* genes).

Studies were excluded, in the following order, if they (i) studied an ineligible disease; (ii) had an ineligible study design, including those that were reviews of evidence (e.g., scoping, systematic, narrative), did not include primary clinical human data, reported data for less than two cases due to an increased risk of selection bias, were incomplete (e.g., ongoing clinical trials), did not report an RNA extraction step before measurement or were studies measuring

medRxiv preprint doi: https://doi.org/10.1101/2020.10.13.20212233; this version posted October 15, 2020. The copyright holder for this preprint
(which was not certified by peer review) is the author/funder, who has granted medRxiv a license to display the preprint in perpetuity.
It is made available under a CC-BY-NC 4.0 International license .

environmental samples; (iii) reported an ineligible metric for specimen concentration (e.g., qualitative RT-PCR or cycle threshold [Ct] values without calibration included in the study); (iv) reported quantitative measurements from an ineligible specimen type (e.g., blood specimens, pooled specimens or self-collected POS or Spu patient specimens in the absence of a healthcare professional); (v) reported an ineligible sampling period (consisted entirely of data that could not be extracted from within the infectious period); or (vi) were duplicates of an included study (e.g., preprinted version of published paper or duplicates not identified by Covidence). We included data from control groups receiving standard of care in interventional studies but excluded data from the intervention group. Patients in the intervention group are, by definition, systematically different from general case populations because they receive therapies not being widely used for treatment, which may influence virus concentrations. Interventional studies examining the comparative effectiveness of two or more treatments were excluded for the same reason. Studies exclusively reporting semiquantitative measurements (e.g., Ct values) of specimen concentration were excluded, as these measurements are sensitive to batch inconsistencies and, without proper calibration, cannot be compared on an absolute scale across studies[34].

We searched, without the use of filters or language restrictions, the following sources: MEDLINE (via Ovid, 1946 to 7 August 2020), EMBASE (via Ovid, 1974 to 7 August 2020, Cochrane Central Register of Controlled Trials (via Ovid, 1991 to 7 August 2020), Web of Science Core Collection (including: Science Citation Index Expanded, 1900 to 7 August 2020; Social Sciences Citation Index, 1900 to 7 August 2020; Arts & Humanities Citation Index, 1975 to 7 August 2020; Conference Proceedings Citation Index - Science, 1990 to 7 August 2020; Conference Proceedings Citation Index - Social Sciences & Humanities, 1990 to 7 August 2020; and Emerging Sources Citation Index, 2015 to 7 August 2020), as well as MedRxiv and BioRxiv

medRxiv preprint doi: https://doi.org/10.1101/2020.10.13.20212233; this version posted October 15, 2020. The copyright holder for this preprint
(which was not certified by peer review) is the author/funder, who has granted medRxiv a license to display the preprint in perpetuity.
It is made available under a CC-BY-NC 4.0 International license .

(both searched through Google Scholar via the Publish or Perish program, to 7 August 2020). We also gathered studies by searching through the reference lists of review articles identified by the database search, by searching through the reference lists of included articles, through expert recommendation (by Epic J. Topol, Akiko Iwasaki and A. Marm Kilpatrick on Twitter) and by hand-searching through journals (*Nature*, *Nat. Med.*, *Science*, *NEJM*, *Lancet*, *Lancet Infect. Dis.*, *JAMA*, *JAMA Intern. Med.* and *BMJ*). A comprehensive search was developed by a librarian, which included subject headings and keywords. The search strategy had 3 main concepts (disease, specimen type and outcome), and each concept was combined using the appropriate Boolean operators. The search was tested against a sample set of known articles that were pre-identified. The line-by-line search strategies for all databases are included in Supplementary Tables 1-5. The search results were exported from each database and uploaded to the Covidence online system for deduplication and screening.

Two authors independently screened titles and abstracts, reviewed full texts, collected data and assessed risk of bias via Covidence and a hybrid critical appraisal checklist based on the Joanna Briggs Institute (JBI) tools for case series, analytical cross-sectional studies and prevalence studies[38-40]. To evaluate the sample size in a study, we used the following calculation:

$$n^* = \frac{z^2\sigma}{d^2}, \quad (1)$$

where n^* is the sample size threshold, z is the z-score for the level of confidence (95%), σ is the standard deviation (assumed to be 3 $\log_{10}$ copies/ml, one quarter of the full range of rVLs) and d is the marginal error (assumed to be 1 $\log_{10}$ copies/ml, based on the minimum detection limit for qRT-PCR across studies)[41]. The hybrid JBI critical appraisal checklist is shown in the Supplementary Notes. Inconsistencies were resolved by discussion and consensus.

medRxiv preprint doi: https://doi.org/10.1101/2020.10.13.20212233; this version posted October 15, 2020. The copyright holder for this preprint (which was not certified by peer review) is the author/funder, who has granted medRxiv a license to display the preprint in perpetuity. It is made available under a CC-BY-NC 4.0 International license .

The search found 27 studies for COVID-19[13,35,42-66], 9 studies for SARS[67-75] and 27 studies for A(H1N1)pdm09[76-102]. Quantitative specimen measurements were collected directly if reported numerically or using WebPlotDigitizer 4.3 (https://apps.automeris.io/wpd/) if reported graphically. For included studies, we also collected the relevant numbers of cases, types of cases, volumes of transport media, pharmacotherapies, DFSO (for symptomatic cases) or day relative to initial laboratory diagnosis (for asymptomatic cases) on which each specimen was taken and numbers of tested specimens. Hospitalized cases were defined as those being tested in a hospital setting and then admitted. Non-admitted cases were defined as those being testing in a hospital setting but not admitted. Community cases were defined as those being tested in a community setting. Symptomatic, presymptomatic and asymptomatic infections were defined as in the study. Based on rare description in the included studies, paucisymptomatic infections, when defined in a study, were included with symptomatic ones. Pediatric cases were defined as those of 18 years of age or lower or as defined in the study. Adult cases were defined as those above 18 years of age or as defined in the study.

Meta-analysis of rVLs

Based on the search design and composition of included studies, the meta-analysis overall estimates were the expected SARS-CoV-2, SARS-CoV-1 and A(H1N1)pdm09 rVL when encountering a COVID-19, SARS or A(H1N1)pdm09 case, respectively, during their infectious period. To determine rVLs, data collected on positive, quantitative specimen measurements were converted to the RNA concentration in the respiratory tract. Viral concentrations in respiratory specimens were denoted as specimen measurements, whereas viral concentrations in the respiratory tract were denoted as rVLs. For example, measurements from swabbed specimens

medRxiv preprint doi: https://doi.org/10.1101/2020.10.13.20212233; this version posted October 15, 2020. The copyright holder for this preprint (which was not certified by peer review) is the author/funder, who has granted medRxiv a license to display the preprint in perpetuity. It is made available under a CC-BY-NC 4.0 International license .

(NPS and OPS) typically report the RNA concentration in viral transport media. Based on the expected uptake volume for swabs (0.128 ± 0.031 ml, mean ± SD)[103] or reported collection volume for expulsed fluid in each study (e.g., 0.5 to 1 ml) along with the reported volume of transport media in each study (e.g., 1 ml), we calculated the dilution factor for each respiratory specimen to estimate the rVLs. If the diluent volume was not reported, then the dilution factor was calculated assuming a volume of 1 ml (NPS and OPS), 2 ml (POS and ETA) or 3 ml (NPA) of transport media[43,45,71]. Unless dilution was reported for Spu specimens, we used the specimen measurement as the rVL[13]. The non-reporting of diluent volume was noted as an element increasing risk of bias in the hybrid JBI critical appraisal checklist. Viral load estimates (based on instrumentation, calibration, procedures and reagents) are not standardized. While the above procedures (including only quantitative measurements after extraction, collecting assay detection limits, correcting for specimen dilution) have considered many of these factors, non-standardization is an inherent limitation in interpreting specimen measurements across studies.

Pooled estimates and 95% CIs for the expected rVL of each virus across their infectious period were calculated using a random-effects meta-analysis. The estimates for rVL assumed that each viral copy was extracted and quantified from the tested specimen aliquot. For studies reporting summary statistics in medians and interquartile or total ranges, we derived estimates of the mean and variance and calculated the 95% CIs[104]. All calculations were performed in units of $\log_{10}$ copies/ml. Between-study heterogeneity in meta-analysis was assessed using the I^2 and τ^2 statistics. The weighting for each study in its virus group was calculated as the reciprocal of the rVL variance.

Subgroup analyses of rVLs

medRxiv preprint doi: https://doi.org/10.1101/2020.10.13.20212233; this version posted October 15, 2020. The copyright holder for this preprint
(which was not certified by peer review) is the author/funder, who has granted medRxiv a license to display the preprint in perpetuity.
It is made available under a CC-BY-NC 4.0 International license .

Subgroup analyses were conducted to compare the expected rVLs of SARS-CoV-2 in adult, pediatric, symptomatic and asymptomatic COVID-19 cases, as previously defined, during the infectious period. The overall estimate for each subgroup was the expected rVL when encountering a case of that subgroup during the infectious period. Studies reporting data exclusively from a subgroup of interest were included in the analysis without modification. For studies in which data for these subgroups constituted only part of its dataset, rVLs from the subgroup were collected to calculate the mean, variance and 95% CIs. All calculations were performed in units of $\log_{10}$ copies/ml. In the analysis, we excluded studies with only a single case in our subgroups of interest. Pooled estimates and 95% CIs for each subgroup were calculated using a random-effects meta-analysis, in which between-study heterogeneity was assessed using the I^2 and τ^2 statistics. The weighting for each study in its subgroup was calculated as the reciprocal of the rVL variance.

Distribution of rVL

To analyze heterogeneity in rVLs, we pooled the entirety of individual sample data (reported as individual specimen measurements rather through descriptive statistics) in the systematic dataset by disease, COVID-19 subgroups and DFSO. For analyses of SARS-CoV-2 dynamics across DFSO, we included estimated rVLs from negative qRT-PCR measurements of respiratory specimens (n=3, 3, 6, 8, 12, 15, 13, 17 and 14 negative specimens for 2, 3, 4, 5, 6, 7, 8, 9 and 10 DFSO, respectively) for cases that had previously been quantitatively confirmed to have COVID-19. These rVLs were estimated based on the reported assay detection limit in the respective study. Probability plots and modified Kolmogorov–Smirnov tests were used to determine the suitability of normal, lognormal, gamma and Weibull distributions to describe the

medRxiv preprint doi: https://doi.org/10.1101/2020.10.13.20212233; this version posted October 15, 2020. The copyright holder for this preprint (which was not certified by peer review) is the author/funder, who has granted medRxiv a license to display the preprint in perpetuity. It is made available under a CC-BY-NC 4.0 International license .

525 distribution of rVLs for SARS-CoV-2, SARS-CoV-1 and A(H1N1)pdm09. For each virus, the
526 data best conformed to Weibull distributions, which is described by the probability density
527 function

528 $$f(v) = \frac{\alpha}{\beta}\left(\frac{v}{\beta}\right)^{\alpha-1} e^{-(v/\beta)^{\alpha}}, \quad (2)$$

529 where α is the shape factor, β is the scale factor and v is rVL ($v \geq 0$ $\log_{10}$ copies/ml). In this
530 distribution, the value of the rVL at the x^{th} percentile was determined using the quantile function,

531 $$v_x = \beta[-\ln(1-x)]^{1/\alpha}. \quad (3)$$

532 For cp curves, we used eq. (3) to determine rVLs from the 1st cp to the 99th cp (step size, 1%).
533 Curve fitting to eq. (2) and calculation of eq. (3) and its 95% CI was performed using the
534 Distribution Fitter application in Matlab R2019b (MathWorks, Inc., Natick, Massachusetts,
535 USA).
536
537 **Meta-regression of *k* and heterogeneity in rVL**
538 To assess the relationship between *k* and heterogeneity in rVL, we performed a univariate meta-
539 regression ($\log k = a(SD) + b$, where a is the slope for association and b is the intercept)
540 between pooled estimates of *k* (based on studies describing community transmission) for
541 COVID-19 (k=0.409)[4-6,105-108], SARS (k=0.165)[17] and A(H1N1)pdm09 (k=8.155)[22,23] and the SD
542 of the rVLs in each study. Since the negative binomial distribution, from which *k* is derived[17], is
543 analogous to a compound Poisson distribution in which each random variable is Log(k)-
544 distributed, the meta-regression was performed with $\log k$. Based on negligible between-study
545 heterogeneity, we used a fixed-effects model. This analysis assumes that the SD of rVLs in each
546 study estimates SD of rVL for the disease. Thus, for weighting in the meta-regression, we used
547 the proportion of rVL samples for each study relative to the entire systematic dataset ($W_i =$

medRxiv preprint doi: https://doi.org/10.1101/2020.10.13.20212233; this version posted October 15, 2020. The copyright holder for this preprint (which was not certified by peer review) is the author/funder, who has granted medRxiv a license to display the preprint in perpetuity. It is made available under a CC-BY-NC 4.0 International license .

548 $n_{\mathrm{i}}/n_{\mathrm{total}}$). The regression line, its 95% CI and its Pearson correlation coefficient (r) were
549 presented along with the p-value for association (meta-regression slope t-test for a) between the
550 two variables. The meta-regression assumed that the viability proportion (for viruses exiting the
551 respiratory tract) was similar across cases for a given respiratory infection; it could be a different
552 value for different diseases. The meta-regression also assumed that the rate profile of particles
553 expelled by respiratory activities (e.g., talking) is similar among the diseases. The limit of
554 detection for qRT-PCR instruments used in the included studies did not significantly affect the
555 analysis of heterogeneity in rVL, as these limits tended to be below the values found for
556 specimens with low virus concentrations.
557
558 **Viral kinetics**
559 To model the kinetics of SARS-CoV-2 rVL, we used a mechanistic epithelial cell-limited model
560 for the respiratory tract[109], based on the system of differential equations:

561 $$\frac{dT}{dt} = -\beta TV \quad (4)$$

562 $$\frac{dI}{dt} = \beta TV - \delta I \quad (5)$$

563 $$\frac{dV}{dt} = pI - cV, \quad (6)$$

564 where T is the number of uninfected target cells, I is the number of productively infected cells, V
565 is the rVL, β is the infection rate constant, p is the rate at which airway epithelial cells shed virus
566 to the extracellular fluid, c is the clearance rate of the virus and δ is the clearance rate of
567 productively infected cells. Parameter units are summarized in Extended Data Table 3. Using
568 these parameters, the viral half-life in the respiratory tract ($t_{1/2} = \ln 2/c$) and the half-life of
569 productively infected cells ($t_{1/2} = \ln 2/\delta$) and their 95% CIs could be estimated. Moreover, the

medRxiv preprint doi: https://doi.org/10.1101/2020.10.13.20212233; this version posted October 15, 2020. The copyright holder for this preprint (which was not certified by peer review) is the author/funder, who has granted medRxiv a license to display the preprint in perpetuity. It is made available under a CC-BY-NC 4.0 International license .

cellular basic reproductive number (the expected number of secondary infected cells from a single productively infected cell placed in a population of susceptible cells) was calculated by

$$R_{0,c} = \frac{p\beta T_0}{c\delta}, \quad (7)$$

where T_0 is the initial number of susceptible cells[109].

For initial parameterization, eqs. (4)-(6) were simplified according to a quasi-steady state approximation[110] to

$$\frac{dT}{dt} = -\beta TV \quad (8)$$

$$\frac{dV}{dt} = rTV - \delta V, \quad (9)$$

where $r = p\beta/c$, for a form with greater numerical stability. The system of differential equations was fitted on the mean estimates of SARS-CoV-2 rVL between -2 and 10 DFSO using the entirety of individual sample data in units of copies/ml. Numerical analysis was implemented using the Fit ODE app in OriginPro 2019b (OriginLab Corporation, Northampton, Massachusetts, USA) via the Runge-Kutta method and initial parameters V_0, I_0 and T_0 of 4 copies/ml, 0 cells and 5×10^7 cells, respectively, for the range -5 to 10 DFSO. The analysis was first performed with eqs. (8)-(9). These output parameters were then used to initialize final analysis using eqs. (4)-(6), where the estimates for β and δ were input as fixed and variable parameters, respectively. The fitted line and its coefficient of determination (r^2) were presented.

To estimate the average incubation period, we extrapolated the kinetic model to 0 and 1 $\log_{10}$ copies/ml pre-symptom onset. To estimate the average duration of shedding, we extrapolated the model to 0 $\log_{10}$ copies/ml post-symptom onset. Unlike experimental estimates, this estimate for duration of shedding was not defined by assay detection limits. These analyses had limitations. To estimate the average DFSO on which SARS-CoV-2 concentration reached

medRxiv preprint doi: https://doi.org/10.1101/2020.10.13.20212233; this version posted October 15, 2020. The copyright holder for this preprint (which was not certified by peer review) is the author/funder, who has granted medRxiv a license to display the preprint in perpetuity. It is made available under a CC-BY-NC 4.0 International license .

592 diagnostic levels, we extrapolated the model pre-symptom onset to the equivalent of 1 and 3
593 $\log_{10}$ copies/ml in specimen concentration (chosen as example assay detection limits), as
594 described by the dilution factor estimation above. The average time from respiratory infection to
595 reach diagnostic levels was then calculated by subtracting these values from the incubation
596 period for 0 $\log_{10}$ copies/ml. However, the extrapolated time for SARS-CoV-2 to reach
597 diagnostic concentrations in the respiratory tract should be validated in tracing studies, in which
598 contacts are prospectively subjected to daily sampling.
599
600 **Considerations for particle dehydration**
601 The desiccation time of a particle in air was described $t_{des} = b^{-1}(d_i^2 - d_{des}^2)$, where b is
602 prefactor for dehydration rate which depends on the environmental conditions, d_i is the initial
603 hydrated diameter and d_{des} is particle diameter after desiccation[111]. After desiccation, the
604 remaining non-volatile matter (ions, molecules, viruses and cells) governs particle size, which is
605 approximately 0.44 times the initial size of particles atomized in the respiratory tract[112].
606 Dehydrated aerodynamic diameter was calculated by $d_a = d_p(\rho/\rho_0)^{1/2}$, where d_p is the
607 dehydrated particle size, ρ is the material density of the respiratory particle and ρ_0 is the
608 reference material density (1 g/cm^3). For conservative estimates, the value of b was taken to be
609 64.9 μm^2/s[113] based on conditions of room temperature and a relative humidity of 59% (near the
610 upper limit of 60% for healthcare and typical indoor specifications)[114]. The equation for
611 desiccation time indicated that respiratory particles begin to dehydrate immediately upon release
612 to the ambient environment. Desiccation occurred rapidly, as the equation estimated that an 11.4-
613 μm particle desiccated to 5 μm in 1.6 s within the model conditions, and this value was an upper
614 limit for the desiccation times of aerosols ($t_{des} \leq 1.6$ s).

medRxiv preprint doi: https://doi.org/10.1101/2020.10.13.20212233; this version posted October 15, 2020. The copyright holder for this preprint (which was not certified by peer review) is the author/funder, who has granted medRxiv a license to display the preprint in perpetuity. It is made available under a CC-BY-NC 4.0 International license .

615

616 **Likelihood of respiratory particles containing virions**

617 To calculate an unbiased estimator for viral partitioning (the expected number of viable copies in
618 an expelled particle at a given size), we multiplied rVLs with the volume equation for spherical
619 particles during atomization and the estimated viability proportion:

620 $$\lambda = \frac{\pi \rho v_p \gamma \upsilon}{6} d^3, \quad (10)$$

621 where λ is the expectation value, ρ is the material density of the respiratory particle (997 g/m^3),
622 v_p is the volumetric conversion factor (1 ml/g), γ is the viability proportion, υ is the rVL and d is
623 the hydrated diameter of the particle during atomization. The model assumed γ was 0.1% for the
624 viruses. For influenza, approximately 0.1% of copies in particles expelled from the respiratory
625 tract represent viable virus[115], which is equivalent to one in 3 $\log_{10}$ copies/ml for rVL or, after
626 dilution in transport media, roughly one in 4 $\log_{10}$ copies/ml for specimen concentration. Recent
627 reports have detected culture-positive respiratory specimens with SARS-CoV-2 concentrations
628 down to 4 $\log_{10}$ copies/ml[13], including from pediatric patients[62] and in the presymptomatic
629 period[15], suggesting the assumption was also suitable for SARS-CoV-2.

630 Likelihood profiles were determined using Poisson statistics, as described by the probability
631 mass function

632 $$\mathrm{P}(X = k) = \frac{\lambda^k e^{-\lambda}}{k!}, \quad (11)$$

633 where k is the number of virions partitioned within the particle. For λ, 95% CIs were determined
634 using the variance of its rVL estimate. To determine 95% CIs for likelihood profiles from the
635 probability mass function, we used the delta method, which specifies

636 $$\mathrm{Var}\big(g(\boldsymbol{\theta})\big) \approx \sigma^2 \dot{g}(\boldsymbol{\theta})' \mathbf{D} \dot{g}(\boldsymbol{\theta}), \quad (12)$$

medRxiv preprint doi: https://doi.org/10.1101/2020.10.13.20212233; this version posted October 15, 2020. The copyright holder for this preprint (which was not certified by peer review) is the author/funder, who has granted medRxiv a license to display the preprint in perpetuity. It is made available under a CC-BY-NC 4.0 International license .

where $\sigma^2\mathbf{D}$ is the covariance matrix of $\boldsymbol{\theta}$ and $\dot{g}(\boldsymbol{\theta})$ is the gradient of $g(\boldsymbol{\theta})$. For the univariate Poisson distribution, $\sigma^2\mathbf{D} = \lambda$ and

$$\dot{g}(\theta) = \frac{\lambda^{k-1}e^{-\lambda}}{k!}(k-\lambda). \quad (13)$$

Based on the relative relationship between the residence time of expelled particles before assessment (~5 s)[116] in the referenced study[115] and the estimated dehydration rates of expelled particles, we took the viability proportion (0.1%) to be for dehydrated particles. The model calculated partitioning of copies using the hydrated volume and then applied the viability proportion for number of virions in particles after emission and dehydration. Thus, we compared likelihoods among expelled, dehydrated particles. In Fig. 4, the comparison between hydrated and dehydrated diameters showed only the relationship in particle size and not the relationship in likelihood of containing viable virus. Based on the scope of the study, the model did not account for the virion half-life as particles deposit onto surfaces or remain suspended in air[117].

Rate profiles of particles expelled by respiratory activities

For the rate profiles of particles expelled during respiratory activities, we used distributions from the literature. For coughing, we considered the rate (particles/cough) of expelling particles at different sizes, as determined by Loudon and Roberts[118], by calculating the mean number of respiratory particles expelled per cough based on subject tests RI, RII, LI, LII and EI (EII was presumed to be an outlier based on the relative rate when compared to EI). These particles were taken to be dehydrated based on the deposition time in the experiment relative to estimated dehydration rates. We compared this rate profile to that of Duguid[119], which were taken to be hydrated particles based on experimental design. For talking, singing and breathing, we obtained data from Morawaska et al[120]. Rate profiles (particles/min) were calculated by converting the

medRxiv preprint doi: https://doi.org/10.1101/2020.10.13.20212233; this version posted October 15, 2020. The copyright holder for this preprint
(which was not certified by peer review) is the author/funder, who has granted medRxiv a license to display the preprint in perpetuity.
It is made available under a CC-BY-NC 4.0 International license .

normalized concentration (particles/cm^3) at each particle size based on normalization (32 channels per decade) for the aerodynamic particle sizer (APS) used, unit conversion (cm^3 to L) and the sample flow rate (1 L/min). Rate profiles of talking and singing were isolated from breathing by subtracting the contribution of breathing to the combined data. Particles were taken to be dehydrated based on the minimum particle age in the measurements. Based on the APS used, the analyzed range for d_a was 0.3-20 μm. While larger droplets may potentially be expelled by the respiratory activities, the data suggested that their emission rates were minimal, and there was a limited bias associated with instrumentation. We compared these data for talking with rate profiles of talking loudly and talking quietly from Asadi et al[121]. For data reported in a size channel, we took the particle size to be the median value. Curves based on discrete particle measurements were connected using the nonparametric Akima spline function.

Shedding virions via respiratory droplets and aerosols

To determine the respiratory shedding rate across particle size, rVL estimates and the hydrated diameters of particles expelled by a respiratory activity were input into eq. (10), and the output was then multiplied by the rate profile of the activity (talking, singing, breathing or coughing). Dehydration and viability considerations were continued from the likelihood models. The model used particle profiles from (coughing) Loudon and Roberts[118] or (talking, singing and breathing) Morawaska et al[120].

To determine the total respiratory shedding rate for a given respiratory activity across cp, we determined the cumulative hydrated volumetric rate (by summing the hydrated volumetric rates across particle sizes for that respiratory activity) and input it into eq. (10). Using rVLs as

medRxiv preprint doi: https://doi.org/10.1101/2020.10.13.20212233; this version posted October 15, 2020. The copyright holder for this preprint (which was not certified by peer review) is the author/funder, who has granted medRxiv a license to display the preprint in perpetuity. It is made available under a CC-BY-NC 4.0 International license .

682 determined by the Weibull quantile functions, we then calculated the Poisson means and their
683 95% CIs at different cps.

684 To assess the relative contribution of aerosols and droplets to mediating respiratory viral
685 shedding for a given respiratory activity, we calculated the proportion of the cumulative hydrated
686 volumetric rate contributed by aerosols ($d_a \leq 5$ μm) or droplets ($d_a > 5$ μm) for that respiratory
687 activity. Since the Poisson mean was proportional to cumulative volumetric rate, this estimate of
688 the relative contribution of aerosols and droplets to respiratory viral shedding was consistent
689 among viruses and cps in the model.

690 In this study, the model for shedding virions via droplets and aerosols did not delineate
691 particles generated in the upper respiratory tract from those generated in the lower respiratory
692 tract, as the sites of atomization remain poorly understood. It also did not differentiate cases with
693 significant expectoration from those without it. In addition, it did not account for individual
694 variation in the profiles of expelled particles; superemitters can expel respiratory particles at
695 rates ~3 times above median[121].
696

697 **Statistical analysis**

698 For data collection, statistical analysis, coding and data visualization, we used Excel v16.40
699 (Microsoft Corporation, Redmond, Washington, USA), OriginPro 2019b (OriginLab
700 Corporation, Northampton, Massachusetts, USA) and Matlab R2019b (MathWorks, Inc., Natick,
701 Massachusetts, USA). Between-study heterogeneity in the random-effects meta-analyses was
702 assessed using the I^2 and τ^2 statistics. Probability plots for normal, lognormal, gamma and
703 Weibull distributions of rVLs were scored based on the Blom method. Modified Kolmogorov-
704 Smirnov tests were used to determine the goodness of fits between rVLs (in $\log_{10}$ copies/ml) and

medRxiv preprint doi: https://doi.org/10.1101/2020.10.13.20212233; this version posted October 15, 2020. The copyright holder for this preprint
(which was not certified by peer review) is the author/funder, who has granted medRxiv a license to display the preprint in perpetuity.
It is made available under a CC-BY-NC 4.0 International license .

normal, lognormal, gamma or Weibull distributions. By accepting the null hypothesis in the modified Kolmogorov–Smirnov test, the given distribution cannot be rejected to fit the data. Based on fitted Weibull distribution parameters, the Weibull quantile function was used to determine the rVL and its 95% CIs at a given cp. The association between *k* and rVL was assessed via meta-regression, and the *p*-value for association was based on the meta-regression slope *t*-test. Likelihood profiles were determined using the Poisson probability mass function and the unbiased estimator for the expected partitioning of virions at a given particle size. Variance on likelihood estimates was determined via the delta method. Since case variance or sample size may be unequal among the viral infections or subgroups, the two-sided Welch's *t*-test was used to compare the difference of expected rVLs in the meta-analysis and subgroup analyses. For all statistical analyses, the significance level (α) was taken to be 0.05.

Data availability

Data will be made available upon request. All raw data, code and model outputs from this study will be made publicly available in online repositories after peer review. Search strategies for the systematic review are shown in Supplementary Tables 1-5. The systematic review protocol was prospectively registered on PROSPERO (registration number, CRD42020204637).

References (for Methods)

36 Moher, D., Liberati, A., Tetzlaff, J., Altman, D. G. & Group, P. Preferred reporting items for systematic reviews and meta-analyses: the PRISMA statement. *PLoS Med.* **6**, e1000097, doi:10.1371/journal.pmed.1000097 (2009).

medRxiv preprint doi: https://doi.org/10.1101/2020.10.13.20212233; this version posted October 15, 2020. The copyright holder for this preprint
(which was not certified by peer review) is the author/funder, who has granted medRxiv a license to display the preprint in perpetuity.
It is made available under a CC-BY-NC 4.0 International license .

37 Higgins, J. P. T. *et al. Cochrane Handbook for Systematic Reviews of Interventions*. (John Wiley & Sons, 2019).

38 Munn, Z. *et al.* Methodological quality of case series studies: an introduction to the JBI critical appraisal tool. *JBI Database System Rev Implement Rep*, doi:10.11124/JBISRIR-D-19-00099 (2019).

39 Moola, S. *et al.* Chapter 7: Systematic reviews of etiology and risk. *JBI Manual for Evidence Synthesis*. (The Joanna Briggs Institute, 2020).

40 Munn, Z., Moola, S., Lisy, K., Riitano, D. & Tufanaru, C. Methodological guidance for systematic reviews of observational epidemiological studies reporting prevalence and cumulative incidence data. *Int. J. Evid. Based Healthc.* **13**, 147-153, doi:10.1097/XEB.0000000000000054 (2015).

41 Johnston, K. M., Lakzadeh, P., Donato, B. M. K. & Szabo, S. M. Methods of sample size calculation in descriptive retrospective burden of illness studies. *BMC Med. Res. Methodol.* **19**, 9, doi:10.1186/s12874-018-0657-9 (2019).

42 Zhang, N. *et al.* Comparative study on virus shedding patterns in nasopharyngeal and fecal specimens of COVID-19 patients. *Sci China Life Sci*, doi:10.1007/s11427-020-1783-9 (2020).

43 Lavezzo, E. *et al.* Suppression of a SARS-CoV-2 outbreak in the Italian municipality of Vo'. *Nature* **584**, 425-429, doi:10.1038/s41586-020-2488-1 (2020).

44 Peng, L. *et al.* SARS-CoV-2 can be detected in urine, blood, anal swabs, and oropharyngeal swabs specimens. *J. Med. Virol.*, doi:10.1002/jmv.25936 (2020).

medRxiv preprint doi: https://doi.org/10.1101/2020.10.13.20212233; this version posted October 15, 2020. The copyright holder for this preprint
(which was not certified by peer review) is the author/funder, who has granted medRxiv a license to display the preprint in perpetuity.
It is made available under a CC-BY-NC 4.0 International license .

748 45 To, K. K. *et al.* Temporal profiles of viral load in posterior oropharyngeal saliva samples
749 and serum antibody responses during infection by SARS-CoV-2: an observational cohort
750 study. *Lancet Infect. Dis.* **20**, 565-574, doi:10.1016/S1473-3099(20)30196-1 (2020).
751 46 Zou, L. *et al.* SARS-CoV-2 viral load in upper respiratory specimens of infected patients.
752 *N. Engl. J. Med.* **382**, 1177-1179, doi:10.1056/NEJMc2001737 (2020).
753 47 Fajnzylber, J. M. *et al.* SARS-CoV-2 viral load is associated with increased disease
754 severity and mortality. Preprinted at medRxiv, doi:10.1101/2020.07.15.20131789 (2020).
755 48 Zheng, S. *et al.* Viral load dynamics and disease severity in patients infected with SARS-
756 CoV-2 in Zhejiang province, China, January-March 2020: retrospective cohort study. *BMJ*
757 **369**, m1443, doi:10.1136/bmj.m1443 (2020).
758 49 Lennon, N. J. *et al.* Comparison of viral levels in individuals with or without symptoms at
759 time of COVID-19 testing among 32,480 residents and staff of nursing homes and assisted
760 living facilities in Massachusetts. Preprinted at medRxiv,
761 doi:10.1101/2020.07.20.20157792 (2020).
762 50 Shrestha, N. K. *et al.* Distribution of transmission potential during nonsevere COVID-19
763 illness. *Clin. Infect. Dis.*, doi:10.1093/cid/ciaa886 (2020).
764 51 Shi, F. *et al.* Association of viral load with serum biomakers among COVID-19 cases.
765 *Virology* **546**, 122-126, doi:10.1016/j.virol.2020.04.011 (2020).
766 52 Hung, I. F. *et al.* Triple combination of interferon beta-1b, lopinavir-ritonavir, and ribavirin
767 in the treatment of patients admitted to hospital with COVID-19: an open-label,
768 randomised, phase 2 trial. *Lancet* **395**, 1695-1704, doi:10.1016/S0140-6736(20)31042-4
769 (2020).

medRxiv preprint doi: https://doi.org/10.1101/2020.10.13.20212233; this version posted October 15, 2020. The copyright holder for this preprint (which was not certified by peer review) is the author/funder, who has granted medRxiv a license to display the preprint in perpetuity. It is made available under a CC-BY-NC 4.0 International license .

53 Iwasaki, S. *et al.* Comparison of SARS-CoV-2 detection in nasopharyngeal swab and saliva. *J. Infect.* **81**, e145-e147, doi:10.1016/j.jinf.2020.05.071 (2020).

54 Perera, R. A. P. M. *et al.* SARS-CoV-2 virus culture from the upper respiratory tract: Correlation with viral load, subgenomic viral RNA and duration of illness. Preprinted at medRxiv, doi:10.1101/2020.07.08.20148783 (2020).

55 Baggio, S. *et al.* SARS-CoV-2 viral load in the upper respiratory tract of children and adults with early acute COVID-19. *Clin. Infect. Dis.*, doi:10.1093/cid/ciaa1157 (2020).

56 Lucas, C. *et al.* Longitudinal analyses reveal immunological misfiring in severe COVID-19. *Nature* **584**, 463-469, doi:10.1038/s41586-020-2588-y (2020).

57 Argyropoulos, K. V. *et al.* Association of initial viral load in severe acute respiratory syndrome coronavirus 2 (SARS-CoV-2) patients with outcome and symptoms. *Am. J. Pathol.* **190**, 1881-1887, doi:10.1016/j.ajpath.2020.07.001 (2020).

58 Mitja, O. *et al.* Hydroxychloroquine for early treatment of adults with mild Covid-19: a randomized-controlled trial. *Clin. Infect. Dis.*, doi:10.1093/cid/ciaa1009 (2020).

59 Vetter, P. *et al.* Daily viral kinetics and innate and adaptive immune responses assessment in COVID-19: a case series. Preprinted at medRxiv, doi:10.1101/2020.07.02.20143271 (2020).

60 Xu, Y. *et al.* Characteristics of pediatric SARS-CoV-2 infection and potential evidence for persistent fecal viral shedding. *Nat. Med.* **26**, 502-505, doi:10.1038/s41591-020-0817-4 (2020).

61 Hurst, J. H. *et al.* SARS-CoV-2 infections among children in the biospecimens from respiratory virus-exposed kids (BRAVE Kids) Study. Preprinted at medRxiv, doi:10.1101/2020.08.18.20166835 (2020).

medRxiv preprint doi: https://doi.org/10.1101/2020.10.13.20212233; this version posted October 15, 2020. The copyright holder for this preprint
(which was not certified by peer review) is the author/funder, who has granted medRxiv a license to display the preprint in perpetuity.
It is made available under a CC-BY-NC 4.0 International license .

793 62 L'Huillier, A. G., Torriani, G., Pigny, F., Kaiser, L. & Eckerle, I. Culture-competent
794 SARS-CoV-2 in nasopharynx of symptomatic neonates, children, and adolescents. *Emerg.*
795 *Infect. Dis.* **26**, 2494-2497, doi:10.3201/eid2610.202403 (2020).
796 63 Han, M. S. *et al.* Viral RNA load in mildly symptomatic and asymptomatic children with
797 COVID-19, Seoul, South Korea. *Emerg. Infect. Dis.* **26**, 2497-2499,
798 doi:10.3201/eid2610.202449 (2020).
799 64 Pan, Y., Zhang, D., Yang, P., Poon, L. L. M. & Wang, Q. Viral load of SARS-CoV-2 in
800 clinical samples. *Lancet Infect. Dis.* **20**, 411-412, doi:10.1016/S1473-3099(20)30113-4
801 (2020).
802 65 Han, M. S. *et al.* Sequential analysis of viral load in a neonate and her mother infected with
803 SARS-CoV-2. *Clin. Infect. Dis.*, doi:10.1093/cid/ciaa447 (2020).
804 66 Kawasuji, H. *et al.* Viral load dynamics in transmissible symptomatic patients with
805 COVID-19. Preprinted at medRxiv, doi:10.1101/2020.06.02.20120014 (2020).
806 67 Chu, C. M. *et al.* Initial viral load and the outcomes of SARS. *CMAJ* **171**, 1349-1352,
807 doi:10.1503/cmaj.1040398 (2004).
808 68 Poon, L. L. *et al.* Early diagnosis of SARS coronavirus infection by real time RT-PCR. *J.*
809 *Clin. Virol.* **28**, 233-238, doi:10.1016/j.jcv.2003.08.004 (2003).
810 69 Chen, W. J. *et al.* Nasopharyngeal shedding of severe acute respiratory syndrome-
811 associated coronavirus is associated with genetic polymorphisms. *Clin. Infect. Dis.* **42**,
812 1561-1569, doi:10.1086/503843 (2006).
813 70 Chu, C. M. *et al.* Role of lopinavir/ritonavir in the treatment of SARS: initial virological
814 and clinical findings. *Thorax* **59**, 252-256, doi:10.1136/thorax.2003.012658 (2004).

medRxiv preprint doi: https://doi.org/10.1101/2020.10.13.20212233; this version posted October 15, 2020. The copyright holder for this preprint
(which was not certified by peer review) is the author/funder, who has granted medRxiv a license to display the preprint in perpetuity.
It is made available under a CC-BY-NC 4.0 International license .

815 71 Poon, L. L. *et al.* Detection of SARS coronavirus in patients with severe acute respiratory
816 syndrome by conventional and real-time quantitative reverse transcription-PCR assays.
817 *Clin. Chem.* **50**, 67-72, doi:10.1373/clinchem.2003.023663 (2004).
818 72 Chu, C. M. *et al.* Viral load distribution in SARS outbreak. *Emerg. Infect. Dis.* **11**, 1882-
819 1886, doi:10.3201/eid1112.040949 (2005).
820 73 Hung, I. F. *et al.* Viral loads in clinical specimens and SARS manifestations. *Emerg. Infect.*
821 *Dis.* **10**, 1550-1557, doi:10.3201/eid1009.040058 (2004).
822 74 Cheng, V. C. *et al.* Viral replication in the nasopharynx is associated with diarrhea in
823 patients with severe acute respiratory syndrome. *Clin. Infect. Dis.* **38**, 467-475,
824 doi:10.1086/382681 (2004).
825 75 Peiris, J. S. *et al.* Clinical progression and viral load in a community outbreak of
826 coronavirus-associated SARS pneumonia: a prospective study. *Lancet* **361**, 1767-1772,
827 doi:10.1016/s0140-6736(03)13412-5 (2003).
828 76 Loeb, M. *et al.* Longitudinal study of influenza molecular viral shedding in Hutterite
829 communities. *J. Infect. Dis.* **206**, 1078-1084, doi:10.1093/infdis/jis450 (2012).
830 77 Suess, T. *et al.* Shedding and transmission of novel influenza virus A/H1N1 infection in
831 households--Germany, 2009. *Am. J. Epidemiol.* **171**, 1157-1164, doi:10.1093/aje/kwq071
832 (2010).
833 78 Li, C. C. *et al.* Correlation of pandemic (H1N1) 2009 viral load with disease severity and
834 prolonged viral shedding in children. *Emerg. Infect. Dis.* **16**, 1265-1272,
835 doi:10.3201/eid1608.091918 (2010).

medRxiv preprint doi: https://doi.org/10.1101/2020.10.13.20212233; this version posted October 15, 2020. The copyright holder for this preprint
(which was not certified by peer review) is the author/funder, who has granted medRxiv a license to display the preprint in perpetuity.
It is made available under a CC-BY-NC 4.0 International license .

79 Lu, P. X. *et al.* Relationship between respiratory viral load and lung lesion severity: a study in 24 cases of pandemic H1N1 2009 influenza A pneumonia. *J. Thorac. Dis.* **4**, 377-383, doi:10.3978/j.issn.2072-1439.2012.08.02 (2012).

80 Ip, D. K. M. *et al.* The dynamic relationship between clinical symptomatology and viral shedding in naturally acquired seasonal and pandemic influenza virus infections. *Clin. Infect. Dis.* **62**, 431-437, doi:10.1093/cid/civ909 (2016).

81 Rath, B. *et al.* Virus load kinetics and resistance development during oseltamivir treatment in infants and children infected with Influenza A(H1N1) 2009 and Influenza B viruses. *Pediatr. Infect. Dis. J.* **31**, 899-905, doi:10.1097/INF.0b013e31825c7304 (2012).

82 Meschi, S. *et al.* Duration of viral shedding in hospitalized patients infected with pandemic H1N1. *BMC Infect. Dis.* **11**, 140, doi:10.1186/1471-2334-11-140 (2011).

83 Wu, U. I., Wang, J. T., Chen, Y. C. & Chang, S. C. Severity of pandemic H1N1 2009 influenza virus infection may not be directly correlated with initial viral load in upper respiratory tract. *Influenza Other Respir. Viruses* **6**, 367-373, doi:10.1111/j.1750-2659.2011.00300.x (2012).

84 Yang, J. R., Lo, J., Ho, Y. L., Wu, H. S. & Liu, M. T. Pandemic H1N1 and seasonal H3N2 influenza infection in the human population show different distributions of viral loads, which substantially affect the performance of rapid influenza tests. *Virus Res.* **155**, 163-167, doi:10.1016/j.virusres.2010.09.015 (2011).

85 Launes, C. *et al.* Viral load at diagnosis and influenza A H1N1 (2009) disease severity in children. *Influenza Other Respir. Viruses* **6**, e89-92, doi:10.1111/j.1750-2659.2012.00383.x (2012).

medRxiv preprint doi: https://doi.org/10.1101/2020.10.13.20212233; this version posted October 15, 2020. The copyright holder for this preprint
(which was not certified by peer review) is the author/funder, who has granted medRxiv a license to display the preprint in perpetuity.
It is made available under a CC-BY-NC 4.0 International license .

858 86 Killingley, B. *et al.* Virus shedding and environmental deposition of novel A (H1N1)
859 pandemic influenza virus: interim findings. *Health Technol. Assess.* **14**, 237-354,
860 doi:10.3310/hta14460-04 (2010).
861 87 Lee, N. *et al.* Viral clearance and inflammatory response patterns in adults hospitalized for
862 pandemic 2009 influenza A(H1N1) virus pneumonia. *Antivir. Ther.* **16**, 237-247,
863 doi:10.3851/IMP1722 (2011).
864 88 Chan, P. K. *et al.* Clinical and virological course of infection with haemagglutinin D222G
865 mutant strain of 2009 pandemic influenza A (H1N1) virus. *J. Clin. Virol.* **50**, 320-324,
866 doi:10.1016/j.jcv.2011.01.013 (2011).
867 89 Hung, I. F. *et al.* Effect of clinical and virological parameters on the level of neutralizing
868 antibody against pandemic influenza A virus H1N1 2009. *Clin. Infect. Dis.* **51**, 274-279,
869 doi:10.1086/653940 (2010).
870 90 To, K. K. *et al.* Delayed clearance of viral load and marked cytokine activation in severe
871 cases of pandemic H1N1 2009 influenza virus infection. *Clin. Infect. Dis.* **50**, 850-859,
872 doi:10.1086/650581 (2010).
873 91 Thai, P. Q. *et al.* Pandemic H1N1 virus transmission and shedding dynamics in index case
874 households of a prospective Vietnamese cohort. *J. Infect.* **68**, 581-590,
875 doi:10.1016/j.jinf.2014.01.008 (2014).
876 92 Ito, M. *et al.* Detection of pandemic influenza A (H1N1) 2009 virus RNA by real-time
877 reverse transcription polymerase chain reaction. *Pediatr. Int.* **54**, 959-962,
878 doi:10.1111/j.1442-200X.2012.03720.x (2012).

medRxiv preprint doi: https://doi.org/10.1101/2020.10.13.20212233; this version posted October 15, 2020. The copyright holder for this preprint
(which was not certified by peer review) is the author/funder, who has granted medRxiv a license to display the preprint in perpetuity.
It is made available under a CC-BY-NC 4.0 International license .

879 93 Li, I. W. *et al.* The natural viral load profile of patients with pandemic 2009 influenza
880 A(H1N1) and the effect of oseltamivir treatment. *Chest* **137**, 759-768,
881 doi:10.1378/chest.09-3072 (2010).
882 94 Esposito, S. *et al.* Viral shedding in children infected by pandemic A/H1N1/2009 influenza
883 virus. *Virol J.* **8**, 349, doi:10.1186/1743-422X-8-349 (2011).
884 95 Lee, C. K. *et al.* Comparison of pandemic (H1N1) 2009 and seasonal influenza viral loads,
885 Singapore. *Emerg. Infect. Dis.* **17**, 287-291, doi:10.3201/eid1702.100282 (2011).
886 96 Cowling, B. J. *et al.* Comparative epidemiology of pandemic and seasonal influenza A in
887 households. *N. Engl. J. Med.* **362**, 2175-2184, doi:10.1056/NEJMoa0911530 (2010).
888 97 To, K. K. *et al.* Viral load in patients infected with pandemic H1N1 2009 influenza A
889 virus. *J. Med. Virol.* **82**, 1-7, doi:10.1002/jmv.21664 (2010).
890 98 Alves, V. R. G. *et al.* Influenza A(H1N1)pdm09 infection and viral load analysis in
891 patients with different clinical presentations. *Mem. Inst. Oswaldo Cruz* **115**, e200009,
892 doi:10.1590/0074-02760200009 (2020).
893 99 Cheng, P. K. *et al.* Performance of laboratory diagnostics for the detection of influenza
894 A(H1N1)v virus as correlated with the time after symptom onset and viral load. *J. Clin.*
895 *Virol.* **47**, 182-185, doi:10.1016/j.jcv.2009.11.022 (2010).
896 100 Ngaosuwankul, N. *et al.* Influenza A viral loads in respiratory samples collected from
897 patients infected with pandemic H1N1, seasonal H1N1 and H3N2 viruses. *Virol J.* **7**, 75,
898 doi:10.1186/1743-422X-7-75 (2010).
899 101 Duchamp, M. B. *et al.* Pandemic A(H1N1)2009 influenza virus detection by real time RT-
900 PCR: is viral quantification useful? *Clin. Microbiol. Infect.* **16**, 317-321,
901 doi:10.1111/j.1469-0691.2010.03169.x (2010).

medRxiv preprint doi: https://doi.org/10.1101/2020.10.13.20212233; this version posted October 15, 2020. The copyright holder for this preprint
(which was not certified by peer review) is the author/funder, who has granted medRxiv a license to display the preprint in perpetuity.
It is made available under a CC-BY-NC 4.0 International license .

902 102 Watanabe, M., Nukuzuma, S., Ito, M. & Ihara, T. Viral load and rapid diagnostic test in
903 patients with pandemic H1N1 2009. *Pediatr. Int.* **53**, 1097-1099, doi:10.1111/j.1442-
904 200X.2011.03489.x (2011).
905 103 Warnke, P., Warning, L. & Podbielski, A. Some are more equal - a comparative study on
906 swab uptake and release of bacterial suspensions. *PLoS One* **9**, e102215,
907 doi:10.1371/journal.pone.0102215 (2014).
908 104 Wan, X., Wang, W., Liu, J. & Tong, T. Estimating the sample mean and standard deviation
909 from the sample size, median, range and/or interquartile range. *BMC Med. Res. Methodol.*
910 **14**, 135, doi:10.1186/1471-2288-14-135 (2014).
911 105 Adam, D. C. *et al.* Clustering and superspreading potential of SARS-CoV-2 infections in
912 Hong Kong. *Nat. Med.*, doi:10.1038/s41591-020-1092-0 (2020).
913 106 Riou, J. & Althaus, C. L. Pattern of early human-to-human transmission of Wuhan 2019
914 novel coronavirus (2019-nCoV), December 2019 to January 2020. *Euro Surveill.* **25**,
915 doi:10.2807/1560-7917.ES.2020.25.4.2000058 (2020).
916 107 Zhang, Y., Li, Y., Wang, L., Li, M. & Zhou, X. Evaluating transmission heterogeneity and
917 super-spreading event of COVID-19 in a metropolis of China. *Int. J. Environ. Res. Public*
918 *Health* **17**, doi:10.3390/ijerph17103705 (2020).
919 108 Tariq, A. *et al.* Real-time monitoring the transmission potential of COVID-19 in
920 Singapore, March 2020. *BMC Med.* **18**, 166, doi:10.1186/s12916-020-01615-9 (2020).
921 109 Baccam, P., Beauchemin, C., Macken, C. A., Hayden, F. G. & Perelson, A. S. Kinetics of
922 influenza A virus infection in humans. *J. Virol.* **80**, 7590-7599, doi:10.1128/JVI.01623-05
923 (2006).

medRxiv preprint doi: https://doi.org/10.1101/2020.10.13.20212233; this version posted October 15, 2020. The copyright holder for this preprint (which was not certified by peer review) is the author/funder, who has granted medRxiv a license to display the preprint in perpetuity. It is made available under a CC-BY-NC 4.0 International license .

924 110 Ikeda, H. *et al.* Quantifying the effect of Vpu on the promotion of HIV-1 replication in the
925 humanized mouse model. *Retrovirology* **13**, 23, doi:10.1186/s12977-016-0252-2 (2016).
926 111 Wells, W. F. On air-borne infection: study II. droplets and droplet nuclei. *Am. J.*
927 *Epidemiol.* **20**, 611-618, doi:10.1093/oxfordjournals.aje.a118097 (1934).
928 112 Nicas, M., Nazaroff, W. W. & Hubbard, A. Toward understanding the risk of secondary
929 airborne infection: emission of respirable pathogens. *J. Occup. Environ. Hyg.* **2**, 143-154,
930 doi:10.1080/15459620590918466 (2005).
931 113 Stadnytskyi, V., Bax, C. E., Bax, A. & Anfinrud, P. The airborne lifetime of small speech
932 droplets and their potential importance in SARS-CoV-2 transmission. *Proc. Natl. Acad.*
933 *Sci. U. S. A.* **117**, 11875-11877, doi:10.1073/pnas.2006874117 (2020).
934 114 Institute, T. F. G. *Guidelines for design and construction of health care facilities*. (The
935 American Institute of Architects, 2006).
936 115 Yan, J. *et al.* Infectious virus in exhaled breath of symptomatic seasonal influenza cases
937 from a college community. *Proc. Natl. Acad. Sci. U. S. A.* **115**, 1081-1086,
938 doi:10.1073/pnas.1716561115 (2018).
939 116 McDevitt, J. J. *et al.* Development and performance evaluation of an exhaled-breath
940 bioaerosol collector for influenza virus. *Aerosol Sci. Technol.* **47**, 444-451,
941 doi:10.1080/02786826.2012.762973 (2013).
942 117 van Doremalen, N. *et al.* Aerosol and surface stability of SARS-CoV-2 as compared with
943 SARS-CoV-1. *N. Engl. J. Med.* **382**, 1564-1567, doi:10.1056/NEJMc2004973 (2020).
944 118 Loudon, R. G. & Roberts, R. M. Droplet expulsion from the respiratory tract. *Am. Rev.*
945 *Respir. Dis.* **95**, 435-442, doi:10.1164/arrd.1967.95.3.435 (1967).

medRxiv preprint doi: https://doi.org/10.1101/2020.10.13.20212233; this version posted October 15, 2020. The copyright holder for this preprint (which was not certified by peer review) is the author/funder, who has granted medRxiv a license to display the preprint in perpetuity. It is made available under a CC-BY-NC 4.0 International license .

946 119 Duguid, J. P. The size and the duration of air-carriage of respiratory droplets and droplet-
947 nuclei. *J. Hyg. (Lond.)* **44**, 471-479, doi:10.1017/s0022172400019288 (1946).
948 120 Morawska, L. *et al.* Size distribution and sites of origin of droplets expelled from the
949 human respiratory tract during expiratory activities. *J. Aerosol Sci* **40**, 256-269,
950 doi:10.1016/j.jaerosci.2008.11.002 (2009).
951 121 Asadi, S. *et al.* Aerosol emission and superemission during human speech increase with
952 voice loudness. *Sci. Rep.* **9**, 2348, doi:10.1038/s41598-019-38808-z (2019).
953

954 **Acknowledgements**

955 We thank T. Alba (Toronto) for discussion on statistical methods. We thank E. Lavezzo and A.
956 Chrisanti (Padova) for responses to data inquiries. This work was supported by the Natural
957 Sciences and Engineering Research Council of Canada (NSERC) and the Toronto COVID-19
958 Action Fund. P.Z.C. was supported by the NSERC Vanier Scholarship (608544). D.N.F. was
959 supported by the Canadian Institutes of Health Research (Canadian COVID-19 Rapid Research
960 Fund, OV4-170360). F.X.G. was supported by the NSERC Senior Industrial Research Chair.
961

962 **Author contributions**

963 P.Z.C. designed the study, performed analyses, interpreted results and drafted the manuscript.
964 P.Z.C. and N.B. conducted screening, appraised studies and drafted the review protocol. Z.P.
965 developed and conducted the systematic review search. M.K. and D.N.F. assessed methods,
966 interpreted results and contributed to the discussion. All authors reviewed and revised the
967 manuscript. F.X.G. secured funds, interpreted results and supervised the project.
968

medRxiv preprint doi: https://doi.org/10.1101/2020.10.13.20212233; this version posted October 15, 2020. The copyright holder for this preprint
(which was not certified by peer review) is the author/funder, who has granted medRxiv a license to display the preprint in perpetuity.
It is made available under a CC-BY-NC 4.0 International license .

969 **Competing interests** The authors declare no competing interests.

970

971 **Supplementary information** is available for this paper.

972

973 **Correspondence and requests for materials** should be addressed to F.X.G.

medRxiv preprint doi: https://doi.org/10.1101/2020.10.13.20212233; this version posted October 15, 2020. The copyright holder for this preprint (which was not certified by peer review) is the author/funder, who has granted medRxiv a license to display the preprint in perpetuity. It is made available under a CC-BY-NC 4.0 International license .

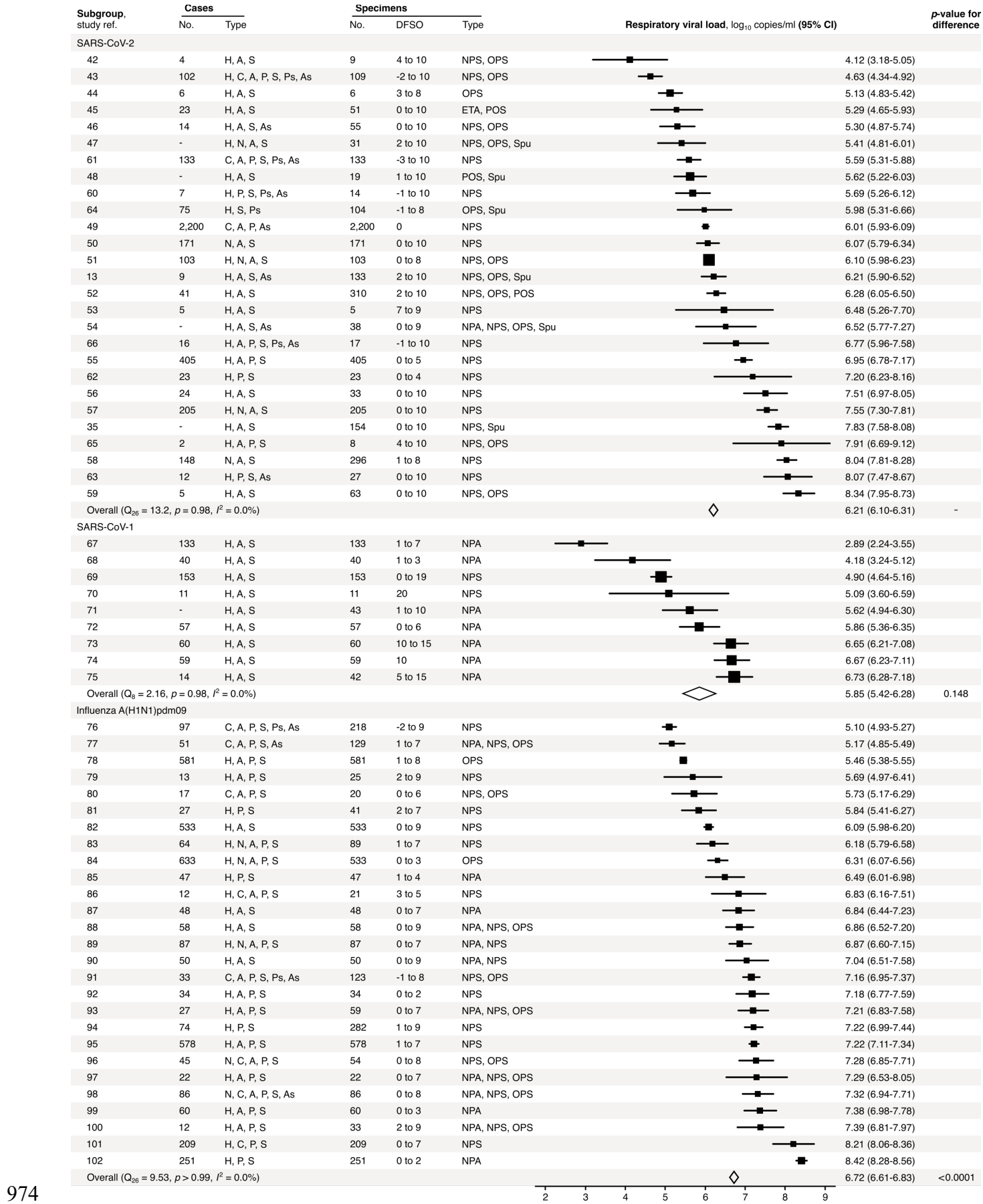

974

medRxiv preprint doi: https://doi.org/10.1101/2020.10.13.20212233; this version posted October 15, 2020. The copyright holder for this preprint
(which was not certified by peer review) is the author/funder, who has granted medRxiv a license to display the preprint in perpetuity.
It is made available under a CC-BY-NC 4.0 International license .

Extended Data Fig. 1. Meta-analysis of respiratory viral loads of SARS-CoV-2, SARS-CoV-1 and influenza A(H1N1)pdm09 during the infectious period. Random-effects meta-analyses comparing the expected rVLs for COVID-19, SARS and A(H1N1)pdm09 cases during the infectious period. Quantitative specimen measurements were used to estimate rVLs, which refer to virus concentrations in the respiratory tract. Case types: hospitalized (H), not admitted (N), community (C), adult (A), pediatric (P), symptomatic (S), presymptomatic (Ps) and asymptomatic (As). Specimen types: endotracheal aspirate (ETA), nasopharyngeal aspirate (NPA), nasopharyngeal swab (NPS), oropharyngeal swab (OPS), posterior oropharyngeal saliva (POS) and sputum (Spu). Studies after ref. 35 are listed in Methods. Dashes denote case numbers that were not obtained. Box sizes are proportional to weighting in the overall estimates. Two-sided Welch's *t*-test (relative to SARS-CoV-2), non-significance ($p>0.05$).

medRxiv preprint doi: https://doi.org/10.1101/2020.10.13.20212233; this version posted October 15, 2020. The copyright holder for this preprint
(which was not certified by peer review) is the author/funder, who has granted medRxiv a license to display the preprint in perpetuity.
It is made available under a CC-BY-NC 4.0 International license .

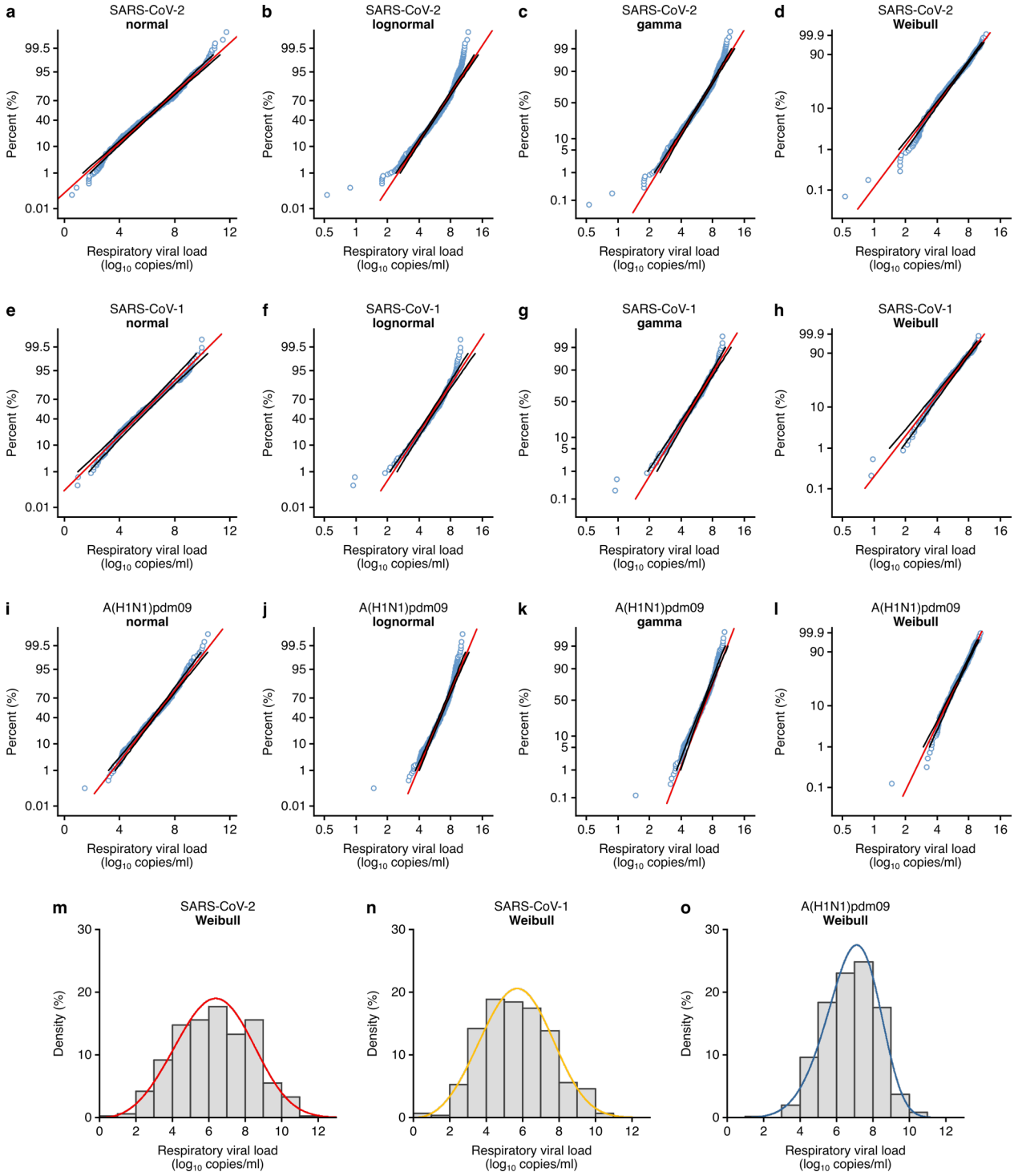

Extended Data Fig. 2. Respiratory viral loads for SARS-CoV-2, SARS-CoV-1 and A(H1N1)pdm09 best conform to Weibull distributions. a-d, Normal ($p \leq 0.01$) (**a**), lognormal ($p \leq 0.01$) (**b**), gamma ($p \leq 0.005$) (**c**) and Weibull ($p > 0.10$, not significant [NS]) (**d**) probability

medRxiv preprint doi: https://doi.org/10.1101/2020.10.13.20212233; this version posted October 15, 2020. The copyright holder for this preprint
(which was not certified by peer review) is the author/funder, who has granted medRxiv a license to display the preprint in perpetuity.
It is made available under a CC-BY-NC 4.0 International license .

plots for individual sample data of SARS-CoV-2 rVLs across DFSO in the systematic dataset (n=916 samples from n=19 studies). **e-h**, Normal (p>0.10, NS) (**e**), lognormal (p≤0.01) (**f**), gamma (p>0.05, NS) (**g**) and Weibull (p>0.10, NS) (**h**) probability plots for individual sample data of SARS-CoV-1 rVLs in the systematic dataset (n=303 samples from n=5 studies). **i-l**, Normal (p≤0.01) (**i**), lognormal (p≤0.01) (**j**), gamma (p≤0.005) (**k**) and Weibull (p>0.10, NS) (**l**) probability plots for individual sample data of A(H1N1)pdm09 rVLs in the systematic dataset (n=512 samples from n=10 studies). These categories included only rVL data from positive (above the detection limit) qRT-PCR measurements. The p-values were determined using the modified Kolmogorov-Smirnov test for the goodness of fit of the distributions. When the null hypothesis is accepted (NS at p>0.05), the probability density function cannot be rejected to describe the distribution of the data. Blue circles, black lines and red lines represent individual sample data, expected distributions and 95% CIs, respectively. **m-o**, Histograms and fitted Weibull distributions of the above data for SARS-CoV-2 (**m**), SARS-CoV-1 (**n**) and A(H1N1)pdm09 (**o**).

medRxiv preprint doi: https://doi.org/10.1101/2020.10.13.20212233; this version posted October 15, 2020. The copyright holder for this preprint
(which was not certified by peer review) is the author/funder, who has granted medRxiv a license to display the preprint in perpetuity.
It is made available under a CC-BY-NC 4.0 International license .

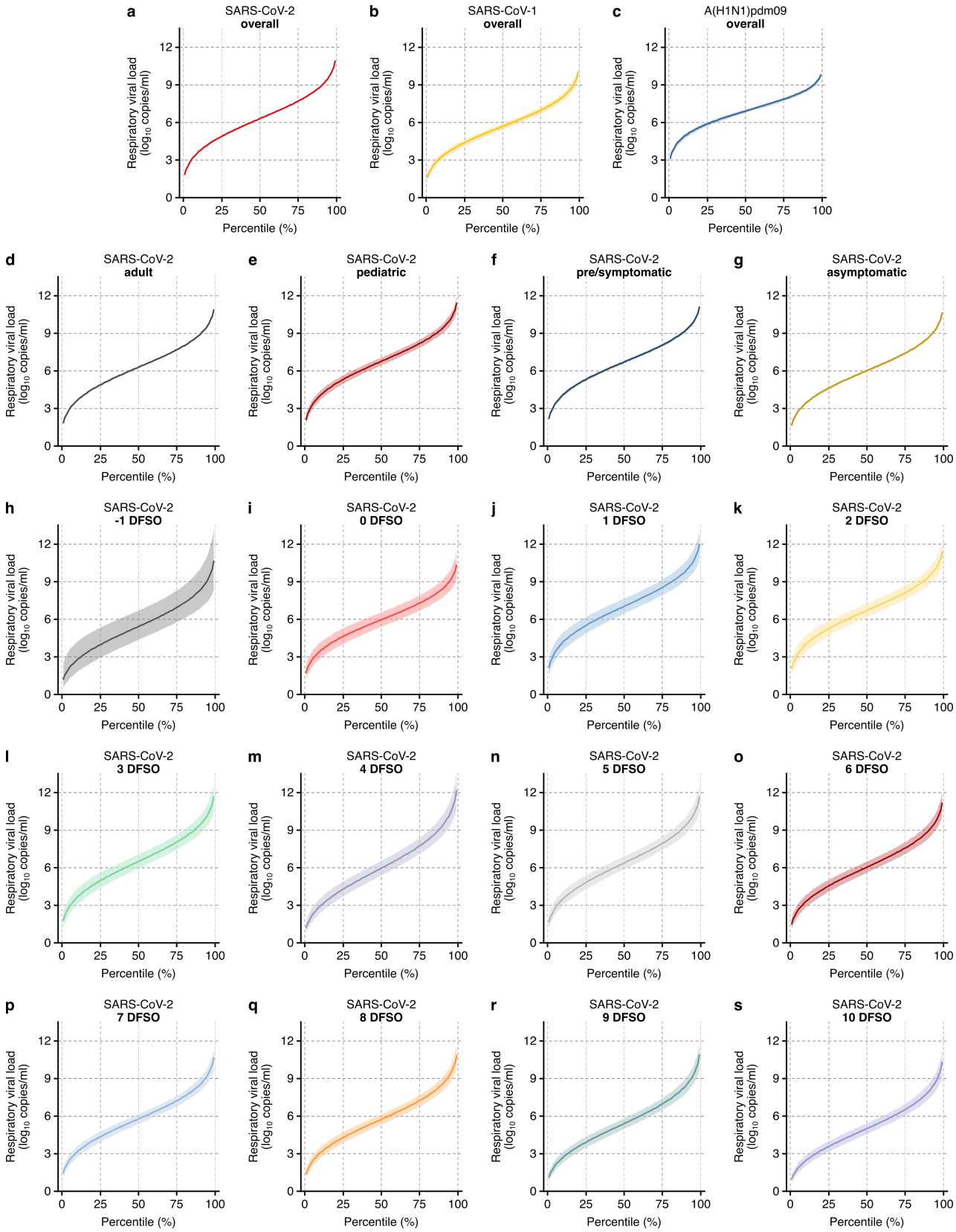

1004

medRxiv preprint doi: https://doi.org/10.1101/2020.10.13.20212233; this version posted October 15, 2020. The copyright holder for this preprint
(which was not certified by peer review) is the author/funder, who has granted medRxiv a license to display the preprint in perpetuity.
It is made available under a CC-BY-NC 4.0 International license .

Extended Data Fig. 3. Respiratory viral loads across case percentiles for viruses, subgroups and days from symptom onset. a, b, Estimated rVLs of SARS-CoV-2 (**a**), SARS-CoV-1 (**b**) and A(H1N1)pdm09 (**c**) across cp during the infectious periods. **d-g**, Estimated SARS-CoV-2 rVLs across cp for adult (**d**), pediatric (**e**), symptomatic/presymptomatic (**f**) and asymptomatic (**g**) cases during the infectious period. **h-s**, Estimated SARS-CoV-2 rVLs across cp on different days of the infectious period. Earlier presymptomatic days were excluded based on limited data. Data ranged between the 1st and 99th cps. Sample numbers, distribution parameters and descriptive statistics are summarized in Extended Data Table 2. Lines and bands represent estimates and 95% CIs, respectively.

medRxiv preprint doi: https://doi.org/10.1101/2020.10.13.20212233; this version posted October 15, 2020. The copyright holder for this preprint
(which was not certified by peer review) is the author/funder, who has granted medRxiv a license to display the preprint in perpetuity.
It is made available under a CC-BY-NC 4.0 International license .

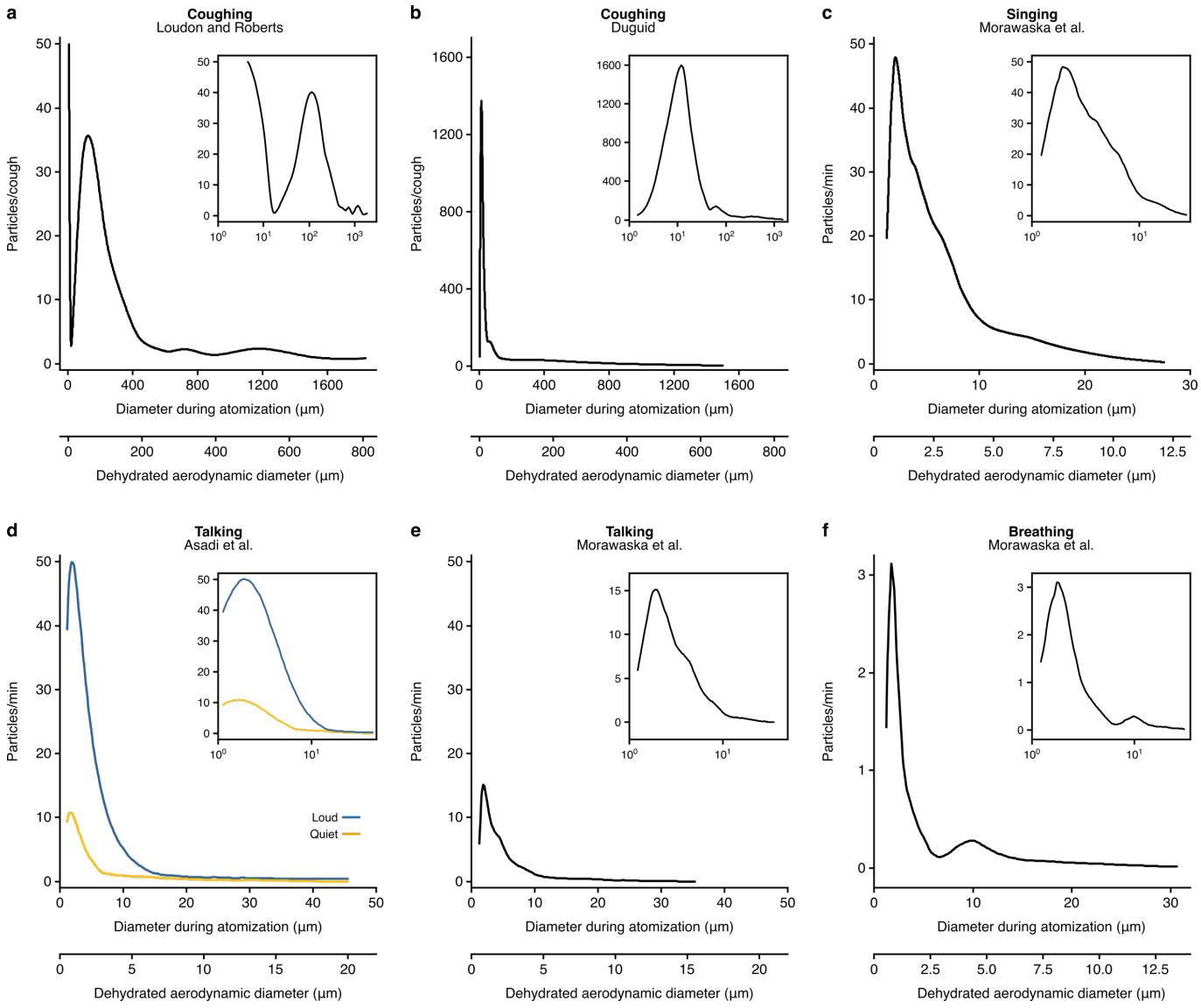

Extended Data Fig. 4. Rate profiles for particle expelled by respiratory activities. a,b, Rate profiles of particles expelled during coughing. The data were obtained from Loudon and Roberts[118] (**a**) and Duguid[119] (**b**). **c**, Rate profile of particles expelled during singing, as obtained from Morawaska et al[120]. **d,e**, Rate profiles of particles expelled during talking. The data were obtained from Asadi et al[121] (**d**) and Morawaska et al[120]. (**e**). **f**, Rate profiles of particles expelled during breathing at a natural pace, as obtained from Morawaska et al[120]. Insets, particle profiles with a logarithmic axis for diameter during atomization.

medRxiv preprint doi: https://doi.org/10.1101/2020.10.13.20212233; this version posted October 15, 2020. The copyright holder for this preprint
(which was not certified by peer review) is the author/funder, who has granted medRxiv a license to display the preprint in perpetuity.
It is made available under a CC-BY-NC 4.0 International license .

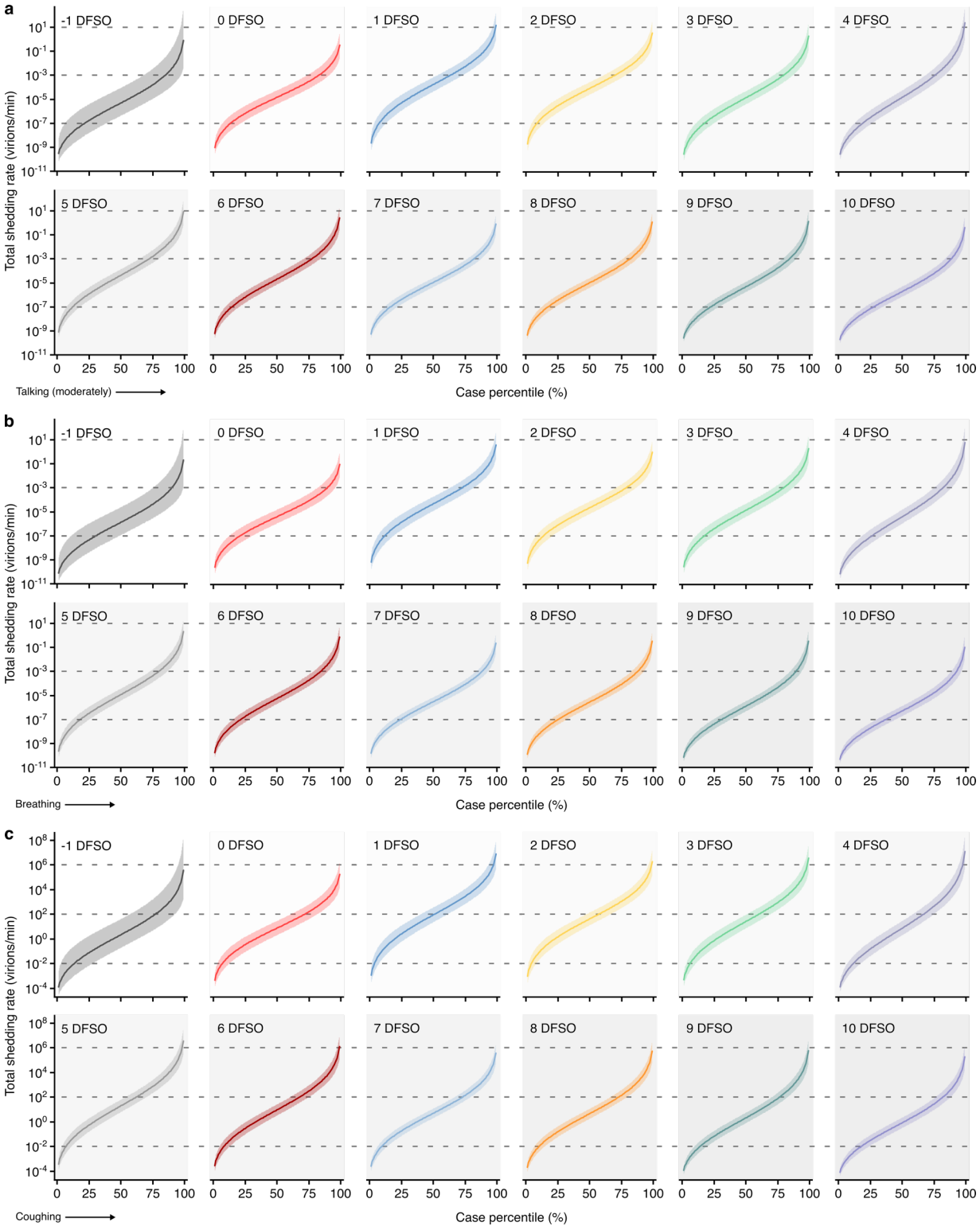

Extended Data Fig. 5. Heterogeneity in shedding SAR-CoV-2 via talking, breathing and coughing. a-c, Case heterogeneity in the total SARS-CoV-2 shedding rate (over all particle

medRxiv preprint doi: https://doi.org/10.1101/2020.10.13.20212233; this version posted October 15, 2020. The copyright holder for this preprint
(which was not certified by peer review) is the author/funder, who has granted medRxiv a license to display the preprint in perpetuity.
It is made available under a CC-BY-NC 4.0 International license .

1025 sizes) by talking at a moderate level (**a**), breathing (**b**) or coughing (**c**) for COVID-19 cases
1026 across the infectious period. Earlier presymptomatic days were excluded based on limited data.
1027 Data represent estimated rates for viable virus and range between the 1st and 99th cps. Lines and
1028 bands represent estimates and 95% CIs, respectively.

medRxiv preprint doi: https://doi.org/10.1101/2020.10.13.20212233; this version posted October 15, 2020. The copyright holder for this preprint
(which was not certified by peer review) is the author/funder, who has granted medRxiv a license to display the preprint in perpetuity.
It is made available under a CC-BY-NC 4.0 International license .

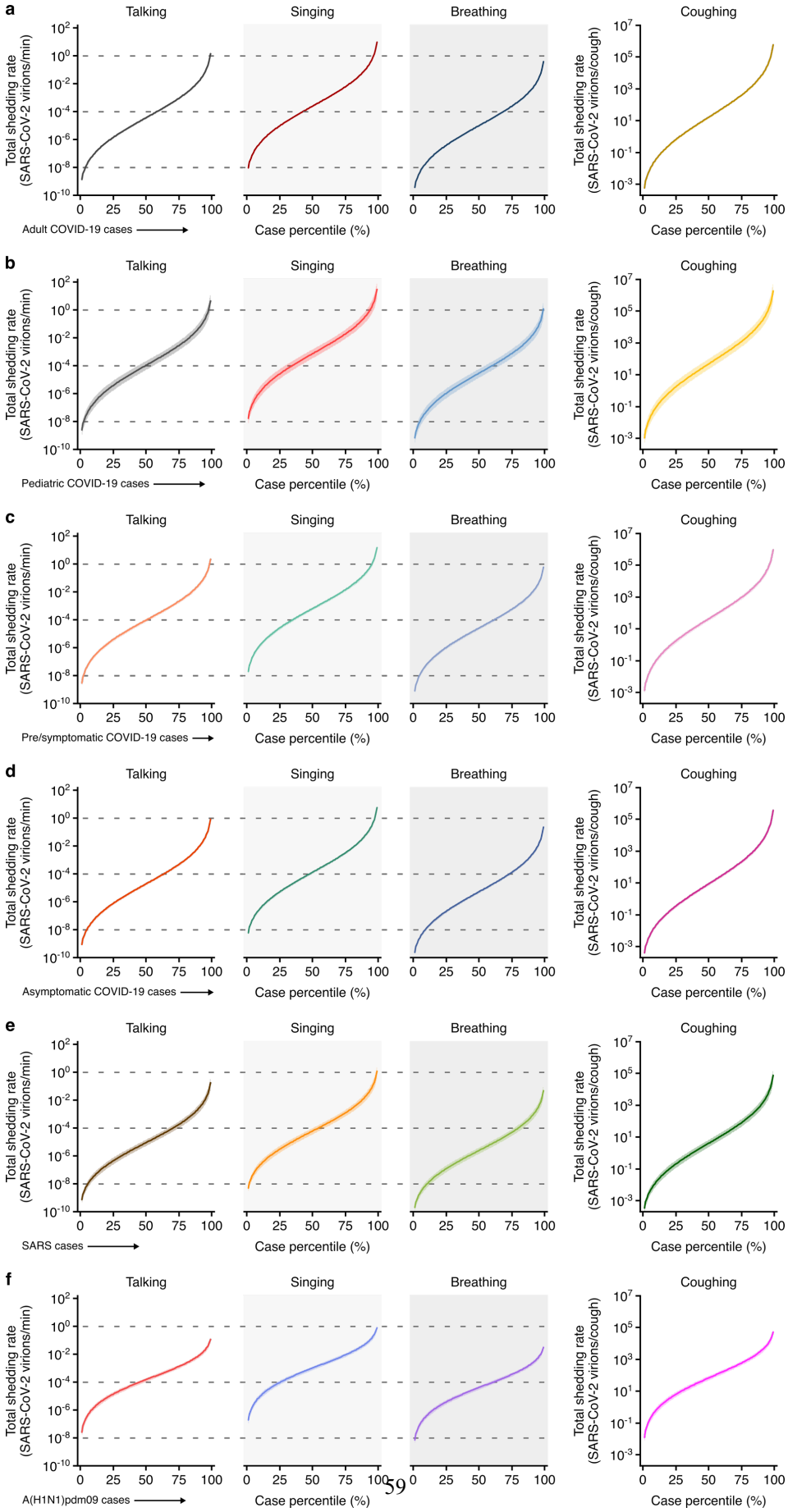

1029

medRxiv preprint doi: https://doi.org/10.1101/2020.10.13.20212233; this version posted October 15, 2020. The copyright holder for this preprint
(which was not certified by peer review) is the author/funder, who has granted medRxiv a license to display the preprint in perpetuity.
It is made available under a CC-BY-NC 4.0 International license .

Extended Data Fig. 6. Heterogeneity in respiratory virus shedding for subgroup COVID-19, SARS and A(H1N1)pdm09 cases. a-d, Case heterogeneity in the total SARS-CoV-2 shedding rate for adult (**a**), pediatric (**b**), symptomatic/presymptomatic (**c**) and asymptomatic (**d**) COVID-19 cases via talking, singing, breathing and coughing during the infectious period. **e,f**, Case heterogeneity in the total SARS-CoV-1 (**e**) and A(H1N1)pdm09 (**f**) shedding rates via talking, singing, breathing and coughing for SARS and A(H1N1)pdm09 cases, respectively, during the infectious periods. Data represent estimated rates for viable virus and range between the 1st and 99th cps. Lines and bands represent estimates and 95% CIs, respectively.

1039 **Extended Data Table 1 | Characteristics of included studies**

Study*	Country	No. of cases included (no. of specimens)	No. of pediatric cases (no. of specimens)	No. of asymptomatic cases (no. of specimens)	Disease caused by virus	Case definition (WHO)	Pharmaco-therapy (type)†	Individual data extracted (diluent volume reported)‡	Adjusted viral load§ (type of specimen)	Weight, % (meta-analysis category)‖	Weight, % (meta-regression)	Risk of bias¶
Argyropoulos et al. (2020)[57]	USA	205 (205)	0	0	COVID-19	Confirmed	No	No (no)	Yes (NPS)	2.3 (V), 2.9 (A), 2.5 (S/Ps)	2.12	********
Baggio et al. (2020)[55]	Switzerland	405 (405)	58 (58)	0	COVID-19	Confirmed	No	Yes (no)	Yes (NPS)	2.1 (V), 2.7 (A), 11.5 (P), 2.2 (S/Ps)	4.18	*******
Fajnzylber et al. (2020)[47]	USA	- (31)	0	0	COVID-19	Confirmed	No	Yes (yes)	Yes (NPS, OPS) No (Spu)	2.8 (V), 3.5 (A), 3.0 (S/Ps)	0.32	********
Han et al. (2020)[65]	South Korea	2 (8)	1 (6)	0	COVID-19	Confirmed	No	Yes (no)	Yes (NPS, OPS)	2.7 (V), 2.8 (S/Ps)	0.08	******
Han et al. (2020)[63]	South Korea	12 (27)	12 (27)	3 (7)	COVID-19	Confirmed	No	Yes (no)	Yes (NPS)	3.2 (V), 18.5 (P), 3.2 (S/Ps), 31.0 (As)	0.28	********
Hung et al. (2020)[52]	China	41 (310)	0	0	COVID-19	Confirmed	No (control group)	No (no)	Yes (NPS, OPS, POS)	2.0 (V), 2.4 (A), 2.1 (S)	3.20	********
Hurst et al. (2020)[61]	USA	133 (133)	54 (54)	52 (52)	COVID-19	Confirmed	No	Yes (no)	Yes (NPS)	2.8 (V), 15.3 (P), 3.0 (S/Ps), 24.1 (As)	1.37	********
Iwasaki et al. (2020)[53]	Japan	5 (5)	0	0	COVID-19	Confirmed	No	Yes (no)	Yes (NPS)	4.2 (V), 5.2 (A), 4.5 (S/Ps)	0.05	***
Kawasuji et al. (2020)[66]	Japan	16 (16)	-	-	COVID-19	Confirmed	Yes (antivirals - type not reported)	Yes (no)	Yes (NPS)	2.8 (V)	0.18	*****
L'Huillier et al. (2020)[62]	Switzerland	23 (23)	23 (23)	0	COVID-19	Confirmed	No	Yes (no)	Yes (NPS)	1.5 (V), 8.4 (P), 1.6 (S/Ps)	0.24	********
Lavezzo et al. (2020)[43]	Italy	103 (110)	2 (3)	49 (49)	COVID-19	Confirmed	No	Yes (yes)	Yes (NPS, OPS)	3.2 (V), 4.0 (A), 14.4 (P), 3.3 (S/Ps), 27.9 (A)	1.13	*******
Lennon et al. (2020)[49]	USA	2,200 (2,200)	18 (18)	2,200 (2,200#)	COVID-19	Confirmed	No	No (yes)	Yes (NPS)	2.0 (V), 2.5 (A), 17.0 (As)	22.70	********
Lucas et al. (2020)[56]	USA	24 (33)	0	0	COVID-19	Confirmed	Moderate and severe patients (tocilizumab)	Yes (yes)	Yes (NPS)	3.3 (V), 4.0 (A), 3.5 (S/Ps)	0.34	*******
Mitja et al. (2020)[58]	Spain	148 (296)	0	0	COVID-19	Confirmed	No (control group)	No (no)	Yes (NPS)	1.9 (V), 2.3 (A), 2.0 (S/Ps)	3.05	********
Pan et al. (2020)[64]	China	75 (104)	-	0	COVID-19	Confirmed	No	Yes (no)	Yes (OPS) No (Spu)	0.7 (V), 0.7 (S/Ps)	1.07	****

Peng et al. (2020)[44]	China	6 (6)	0	0	COVID-19	Confirmed	Yes (arbidol, lopinavir, ritonavir)	Yes (no)	Yes (OPS)	6.6 (V), 8.2 (A), 7.1 (S/Ps)	0.06	********
Perera et al. (2020)[54]	China	- (36)	0	-	COVID-19	Confirmed	No	Yes (no)	Yes (NPA, NPS, OPS, Spu)	1.5 (V), 1.8 (A)	0.39	****
Shi et al. (2020)[51]	China	103 (103)	0	0	COVID-19	Confirmed	No	Yes (no)	Yes (NPS, OPS)	19.0 (V), 23.4 (A), 20.2 (S/Ps)	1.06	*****
Shrestha et al. (2020)[50]	USA	171 (171)	0	0	COVID-19	Confirmed	No	Yes (no)	Yes (NPS)	2.4 (V), 3.0 (A), 2.6 (S/Ps)	1.76	*******
To et al. (2020)[45]	China	23 (51)	0	0	COVID-19	Confirmed	No	Yes (yes)	Yes (ETA, POS)	1.5 (V), 1.8 (A), 1.6 (S/Ps)	0.53	*********
van Kampen et al. (2020)[35]	The Netherlands	- (154)	0	0	COVID-19	Confirmed	No	Yes (yes)	Yes (NPS, Spu)	3.2 (V), 4.0 (A), 3.5 (S/Ps)	1.59	*******
Vetter et al. (2020)[59]	Switzerland	5 (63)	0	0	COVID-19	Confirmed	No	Yes (yes)	Yes (NPS, OPS)	3.3 (V), 4.1 (A), 3.5 (S/Ps)	0.65	*********
Wölfel et al. (2020)[13]	Germany	9 (136)	0	1 (4)	COVID-19	Confirmed	No	Yes (yes)	Yes (NPS, OPS) No (Spu)	2.5 (V), 3.0 (A), 3.2 (S)	1.37	*******
Xu et al. (2020)[60]	China	7 (14)	7 (14)	1 (1)	COVID-19	Confirmed	No	Yes (no)	Yes (NPS)	5.5 (V), 31.8 (P), 5.8 (S/Ps),	0.14	********
Zhang et al. (2020)[42]	China	9 (9)	0	0	COVID-19	Confirmed	No	Yes (no)	Yes (NPS, OPS)	4.0 (V), 5.0 (A), 4.3 (S/Ps)	0.09	********
Zheng et al. (2020)[48]	China	- (19)	0	0	COVID-19	Confirmed	No	Yes (no)	Yes (POS, Spu)	10.0 (V), 12.4 (A), 10.7 (S/Ps)	0.20	*******
Zou et al. (2020)[46]	China	14 (55)	0	1 (4)	COVID-19	Confirmed	No	Yes (no)	Yes (NPS, OPS)	3.0 (V), 3.7 (A), 3.1 (S/Ps)	0.57	********
Chen et al. (2006)[69]	China	154 (154#)	0	0	SARS	Confirmed	Yes (oseltamivir, broad-spectrum antibiotics, ribavirin)	Yes (no)	Yes (NPS)	17.9 (V)	1.58	********
Chu et al. (2004)[67]	China	133 (133)	0	0	SARS	Confirmed	No	No (yes)	Yes (NPA)	2.9 (V)	1.37	*********
Chu et al. (2004)[70] ☆	China	11 (11)	0	0	SARS	Confirmed	No (control group)	Yes (yes)	Yes (NPS)	6.7 (V)	0.11	*********
Chu et al. (2005)[72]	China	57 (57)	0	0	SARS	Confirmed	No	Yes (yes)	Yes (NPA)	11.6 (V)	0.59	*********
Cheng et al. (2004)[74]	China	59 (59)	0	0	SARS	Confirmed	Yes (ribavirin, hydrocortisone, prednisolone, methylpredni-solone)	Yes (yes)	Yes (NPA)	14.2 (V)	0.61	********
Hung et al. (2004)[73]	China	60 (60)	0	0	SARS	Confirmed	Yes (ribavirin, hydrocortisone, prednisolone,	No (yes)	Yes (NPA)	14.7 (V)	0.62	*******

							methylpredni-solone)					
Peiris et al. (2003)[75] ☆	China	14 (42)	0	0	SARS	Confirmed	Yes (ribavirin, hydrocortisone, prednisolone, methylpredni-solone)	Yes (no)	Yes (NPA)	19.2 (V)	0.43	********
Poon et al. (2003)[68]	China	40 (40)	0	0	SARS	Confirmed	No	No (yes)	Yes (NPA)	4.6 (V)	0.41	*****
Poon et al. (2004)[71]	China	- (43)	0	0	SARS	Confirmed	-	No (yes)	Yes (NPA)	8.2 (V)	0.44	*****
Alves et al. (2020)[98]	Brazil	86 (86)	-	15 (15)	Influenza A(H1N1)pdm09	Confirmed	No	No (yes)	Yes (NPA, NPS, OPS)	2.4 (V)	0.89	*****
Chan et al. (2011)[88]	China	58 (58)	0	0	Influenza A(H1N1)pdm09	Confirmed	No (pretreatment)	Yes (no)	Yes (NPA, NPS, OPS)	4.6 (V)	0.60	******
Cheng et al. (2010)[99]	China	60 (60)	-	0	Influenza A(H1N1)pdm09	Confirmed	No (pretreatment)	No (no)	Yes (NPA)	3.3 (V)	0.62	******
Cowling et al. (2010)[96]	China	45 (54)	22 (31)	0	Influenza A(H1N1)pdm09	Confirmed	Yes (22 cases on oseltamivir)	Yes (yes)	Yes (NPS, OPS)	3.1 (V)	0.56	*******
Duchamp et al. (2010)[101]	France	209 (209)	209 (209)	0	Influenza A(H1N1)pdm09	Confirmed	Yes (oseltamivir, zanamivir)	No (yes)	Yes (NPS)	2.4 (V)	2.16	*****
Esposito et al. (2011)[94]	Italy	74 (282)	74 (282)	0	Influenza A(H1N1)pdm09	Confirmed	No	Yes (yes)	Yes (NPS)	2.2 (V)	2.91	******
Hung et al. (2010)[89]	China	87 (87)	-	0	Influenza A(H1N1)pdm09	Confirmed	Yes (oseltamivir)	Yes (no)	Yes (NPA, NPS)	4.7 (V)	0.90	******
Ip et al. (2016)[80]	China	17 (20)	7 (-)	0	Influenza A(H1N1)pdm09	Confirmed	No	Yes (no)	Yes (NPS, OPS)	5.0 (V)	0.21	******
Ito et al. (2012)[92]	Japan	34 (34)	-	0	Influenza A(H1N1)pdm09	Confirmed	No (pretreatment)	Yes (yes)	Yes (NPS)	5.5 (V)	0.35	*****
Killingley et al. (2010)[86]	United Kingdom	12 (21)	-	0	Influenza A(H1N1)pdm09	Confirmed	Yes (oseltamivir)	Yes (yes)	Yes (NPS)	3.3 (V)	0.22	********
Launes et al. (2012)[85]	Spain	47 (47)	47 (47)	0	Influenza A(H1N1)pdm09	Confirmed	No (pretreatment)	No (no)	Yes (NPA)	3.0 (V)	0.48	*******
Lee et al. (2011)[87]	China	48 (48)	0	0	Influenza A(H1N1)pdm09	Confirmed	No (pretreatment)	No (no)	Yes (NPA)	4.1 (V)	0.50	******
Lee et al. (2011)[95]	Singapore	578 (578)	231 (231)	0	Influenza A(H1N1)pdm09	Confirmed	No (pretreatment)	No (no)	Yes (NPS)	4.1 (V)	5.96	*********
Li et al. (2010)[78]	China	581 (581)	522 (522)	0	Influenza A(H1N1)pdm09	Confirmed	No (pretreatment)	No (no)	Yes (OPS)	6.7 (V)	5.99	******
Li et al. (2010)[93]	China	27 (59)	-	0	Influenza A(H1N1)pdm09	Confirmed	No (non-treated group)	No (no)	Yes (NPA, NPS, OPS)	3.8 (V)	0.61	*******
Loeb et al. (2012)[76]	Canada	97 (218)	-	- (17)	Influenza A(H1N1)pdm09	Confirmed	No	No (no)	Yes (NPS)	4.9 (V)	2.25	*******

Lu et al. (2012)[79]	China	13 (25)	-	0	Influenza A(H1N1)pdm09	Confirmed	Yes (oseltamivir, zanamivir)	Yes (no)	Yes (NPS)	2.4 (V)	0.26	*******
Meschi et al. (2011)[82]	Italy	533 (533)	0	0	Influenza A(H1N1)pdm09	Confirmed	No (pretreatment)	No (no)	Yes (NPS)	4.8 (V)	5.50	*********
Ngaosuwankul et al. (2010)[100]	China	12 (33)	-	0	Influenza A(H1N1)pdm09	Confirmed	No (pretreatment)	No (yes)	Yes (NPA, NPS, OPS)	2.8 (V)	0.34	******
Rath et al. (2012)[81]	Germany	27 (41)	27 (41)	0	Influenza A(H1N1)pdm09	Confirmed	Yes (oseltamivir)	Yes (yes)	Yes (NPS)	4.1 (V)	0.42	*********
Suess et al. (2010)[77]	Germany	51 (129)	12 (-)	1 (1)	Influenza A(H1N1)pdm09	Confirmed	Yes (oseltamivir)	No (no)	Yes (NPA, NPS, OPS)	2.4 (V)	1.33	******
Thai et al. (2014)[91]	Vietnam	33 (123)	16 (-)	5 (28)	Influenza A(H1N1)pdm09	Confirmed	Yes (oseltamivir)	Yes (yes)	Yes (NPS)	5.8 (V)	1.27	*******
To et al. (2010)[90]	China	50 (50)	0	0	Influenza A(H1N1)pdm09	Confirmed	Yes (oseltamivir, nebulized zanamivir)	No (no)	Yes (NPA, NPS)	2.2 (V)	0.52	******
To et al. (2010)[97]	China	22 (22)	-	0	Influenza A(H1N1)pdm09	Confirmed	No (pretreatment)	No (no)	Yes (NPA, NPS, OPS)	2.5 (V)	0.23	*****
Watanabe et al. (2011)[102]	Japan	251 (251)	251 (251)	0	Influenza A(H1N1)pdm09	Confirmed	No (pretreatment)	No (yes)	Yes (NPA)	6.6 (V)	2.59	**********
Wu et al. (2012)[83]	China	64 (89)	-	0	Influenza A(H1N1)pdm09	Confirmed	Yes (oseltamivir)	No (yes)	Yes (NPS)	2.3 (V)	0.92	******
Yang et al. (2011)[84]	China	251 (251)	-	0	Influenza A(H1N1)pdm09	Confirmed	N/A	No (yes)	Yes (OPS)	0.8 (V)	6.53	******

*References 13 and 35 are listed in the main body while those 42 and after are listed in Methods. Data shown as "-" were not obtained from the paper or authors.

†Responses of "no" for pharmacotherapy are based on no pharmacotherapy given to any patients or none reported in the study.

‡For studies reporting specimen measurements as individual sample data (either in numerical or graphical formats), the sample data was extracted for analysis.

§Specimen measurements were converted to rVLs based on the dilution factor for specimens immersed in transport media.

‖Abbreviations: viral meta-analysis (V), adult subgroup (A), pediatric subgroup (P), symptomatic/presymptomatic subgroup (S/Ps), asymptomatic subgroup (As).

¶The hybrid JBI Critical Appraisal Checklist was used, with more stars indicating lower risk of bias. Results from each study are shown in Supplementary Table 6.

#For these studies, only 2,147 (Lennon et al.) and 134 (Chen et al.) individual specimen measurements were obtained for the individual sample datasets.

☆For Chu et al., only specimen measurements at 20 DFSO were extracted, as 5-15 DFSO were equivalent specimens as those reported in Peiris et al.

Extended Data Table 2 | Descriptive parameters for subgroups of respiratory viral loads based on individual sample data

			Weibull distribution parameters		Respiratory viral load, log_{10} copies/ml				
Category	***n*** * **(specimens)**	***n*** * **(studies)**	**Scale factor (95% CI)**	**Shape factor (95% CI)**	**Mean (95% CI)**†	**SD**†	**90th percentile (95% CI)**‡	**95th percentile (95% CI)**‡	**99th percentile (95% CI)**‡
SARS-CoV-2 (overall)§	3,778	24	7.01 (6.94-7.07)	3.47 (3.38-3.56)	6.28 (6.22-6.35)	2.04	8.91 (8.82-9.00)	9.61 (9.51-9.71)	10.88 (10.75-11.02)
SARS-CoV-1 (overall)§	303	5	6.34 (6.12-6.56)	3.37 (3.09-3.68)	5.69 (5.48-5.90)	1.86	8.11 (7.83-8.40)	8.77 (8.45-9.11)	9.96 (9.54-10.41)
A(H1N1)pdm09 (overall)§	512	10	7.39 (7.27-7.51)	5.43 (5.07-5.81)	6.81 (6.69-6.94)	1.45	8.62 (8.47-8.76)	9.04 (8.88-9.21)	9.79 (9.59-10.00)
SARS-CoV-2 (adult)§	3,532	18	6.99 (6.92-7.06)	3.47 (3.38-3.56)	6.27 (6.20-6.34)	2.04	8.89 (8.80-8.98)	9.59 (9.49-9.70)	10.86 (10.72-11.00)
SARS-CoV-2 (pediatric)§	185	7	7.47 (7.17-7.79)	3.65 (3.26-4.08)	6.73 (6.43-7.02)	2.06	9.39 (9.01-9.79)	10.09 (9.65-10.56)	11.36 (10.78-11.97)
SARS-CoV-2 (symptomatic/presymptomatic)§	1,503	20	7.39 (7.28-7.49)	3.79 (3.64-3.94)	6.66 (6.56-6.76)	2.01	9.21 (9.08-9.34)	9.87 (9.72-10.02)	11.06 (10.86-11.26)
SARS-CoV-2 (asymptomatic)§	2,212	6	6.72 (6.63-6.81)	3.32 (3.22-3.44)	6.01 (5.93-6.09)	2.02	8.64 (8.52-8.75)	9.35 (9.21-9.48)	10.64 (10.46-10.81)
SARS-CoV-2 (all DFSO)§	916	19	7.04 (6.90-7.18)	3.47 (3.30-3.65)	6.32 (6.19-6.45)	2.04	8.95 (8.78-9.13)	9.66 (9.45-9.86)	10.93 (10.66-11.21)
SARS-CoV-2 (-3 DFSO)‖	1	1	-	-	10.34	-	-	-	-
SARS-CoV-2 (-2 DFSO)‖	3	2	-	-	4.22 (2.41-6.02)	1.59	-	-	-
SARS-CoV-2 (-1 DFSO)	15	5	6.17 (5.11-7.47)	2.82 (1.89-4.19)	5.48 (4.25-6.70)	2.21	8.30 (6.88-10.02)	9.11 (7.44-11.16)	10.62 (8.38-13.45)
SARS-CoV-2 (0 DFSO)	48	10	6.63 (6.08-7.23)	3.46 (2.81-4.26)	5.97 (5.43-6.51)	1.85	8.43 (7.75-9.18)	9.10 (8.32-9.96)	10.31 (9.29-11.43)
SARS-CoV-2 (1 DFSO)	59	10	7.79 (7.23-8.40)	3.58 (2.91-4.40)	7.00 (6.42-7.59)	2.26	9.83 (9.12-10.61)	10.58 (9.75-11.49)	11.93 (10.84-13.14)
SARS-CoV-2 (2 DFSO)¶	69	13	7.42 (6.93-7.95)	3.61 (2.97-4.39)	6.67 (6.15-7.19)	2.17	9.35 (8.72-10.03)	10.06 (9.32-10.85)	11.33 (10.35-12.40)
SARS-CoV-2 (3 DFSO)¶	71	15	7.27 (6.74-7.84)	3.25 (2.69-3.93)	6.50 (5.96-7.04)	2.29	9.39 (8.71-10.14)	10.19 (9.38-11.06)	11.63 (10.54-12.82)
SARS-CoV-2 (4 DFSO)¶	81	15	6.84 (6.27-7.45)	2.66 (2.22-3.17)	6.08 (5.52-6.63)	2.51	9.36 (8.58-10.21)	10.34 (9.40-11.36)	12.15 (10.87-13.59)
SARS-CoV-2 (5 DFSO)¶	87	14	7.16 (6.67-7.68)	3.14 (2.65-3.72)	6.40 (5.91-6.89)	2.29	9.33 (8.69-10.02)	10.15 (9.40-10.96)	11.64 (10.63-12.74)
SARS-CoV-2 (6 DFSO)¶	102	14	6.81 (6.37-7.27)	3.09 (2.63-3.62)	6.07 (5.63-6.51)	2.24	8.92 (8.34-9.53)	9.71 (9.03-10.44)	11.16 (10.24-12.17)
SARS-CoV-2 (7 DFSO)¶	125	18	6.50 (6.13-6.89)	3.10 (2.69-3.58)	5.82 (5.45-6.19)	2.10	8.50 (8.01-9.03)	9.26 (8.67-9.88)	10.63 (9.84-11.49)
SARS-CoV-2 (8 DFSO)¶	119	18	6.49 (6.09-6.91)	2.99 (2.59-3.46)	5.79 (5.40-6.18)	2.14	8.57 (8.04-9.13)	9.35 (8.73-10.02)	10.80 (9.96-11.71)
SARS-CoV-2 (9 DFSO)¶	117	18	6.18 (5.76-6.63)	2.72 (2.35-3.15)	5.51 (5.11-5.91)	2.20	8.40 (7.82-9.01)	9.25 (8.57-9.98)	10.83 (9.90-11.85)
SARS-CoV-2 (10 DFSO)¶	110	16	5.76 (5.34-6.20)	2.61 (2.25-3.03)	5.13 (4.73-5.53)	2.11	7.92 (7.34-8.55)	8.76 (8.07-9.51)	10.33 (9.38-11.37)

*These two columns summarize the cumulative number of specimens (left) collected from the number of studies (right) for each category in the systematic dataset.
†The mean and sample SD were calculated on the entire set of individual sample data for each category.
‡The Weibull quantile distributions were used to determine rVLs at the 90th, 95th and 99th cps.
§These categories included only rVL data from positive (above the detection limit) qRT-PCR measurements.
‖Data for earlier DFSO were excluded from distribution fitting based on limited data, and empty cells were marked with "-".
¶These categories included negative qRT-PCR measurements (set at the detection limit to estimate rVLs; *n* = 3, 3, 6, 8, 12, 15, 13, 17 and 14 specimens for 2-10 DFSO, respectively) for cases that tested positive at an earlier DFSO.

medRxiv preprint doi: https://doi.org/10.1101/2020.10.13.20212233; this version posted October 15, 2020. The copyright holder for this preprint
(which was not certified by peer review) is the author/funder, who has granted medRxiv a license to display the preprint in perpetuity.
It is made available under a CC-BY-NC 4.0 International license .

Extended Data Table 3 | Model parameters describing SARS-CoV-2 kinetics in the respiratory tract

Parameter	Description	Value (95% CI)	Units
β	Infection rate constant	4.02 (3.01-5.03)	$\times 10^{-7}$ (copies/ml)$^{-1}$ day^{-1}
p	Cellular shedding rate of virus	1.11 (0.51-1.71)	copies/ml day^{-1} cell^{-1}
c	Clearance rate of virus	3.82 (0.17-7.47)	day^{-1}
δ	Clearance rate of infected epithelial cells	0.55 (0.23-0.87)	day^{-1}
$R_{0,c}$	Cellular basic reproductive number	10.6	unitless
V_0*	Initial rVL parameter	4	copies/ml
I_0*	Initial number of infected cells	0	cells
T_0*	Initial number of uninfected cells	5×10^7	cells

*Initial values were used as inputs for the numerical estimation of the model parameters.